*Supporting information*

# Polymorphism of R-encenicline hydrochloride: access to the highest number of structurally characterized polymorphs using desolvation of various solvates

*Artis Kons[a]*, Agris Bērziņš[a], Andris Actiņš[a], Toms Rekis[b] and Sander van Smaalen[b] and Anatoly Mishnev[c]*

*[a]Faculty of Chemistry, University of Latvia, Jelgavas iela 1, Riga, LV1004, Latvia*
*[b]Laboratory of Crystallography, University of Bayreuth 95440 Bayreuth, Germany*
*[c] Latvian Institute of Organic Synthesis, 21 Aizkraukles Street, Riga, LV-1006, Latvia*
*artis.kons@lu.lv

Table of Contents SI

1. Solvate screening SI
2. Thermal Characterization and VT-PXRD. SI
3. Monohydrate MH-V and MH-VI characterization
4. Crystal structure determination SI
5. Conformation analysis SI
6. Packing analysis SI
7. Thermal characterization SI

## SI 1. Solvate screening

**Table S1.** Solvates obtained in solid form screening, their lattice parameters and grouping according to identified isomorphism/isostructurality.

| type | solvent | space group | a. Å | b. Å | c. Å | β. ° | V. Å³ | stochio-metry | desolvation product |
|---|---|---|---|---|---|---|---|---|---|
| 1. | isobutanol | $P_{212121}$ | 26.53 | 12.16 | 6.69 | 90 | 2160 | 1:1 | $V_D$ |
| | chloroform | | 26.08 | 12.15 | 6.69 | | 2119 | 1:1 | $V_D$ |
| | trifluoroethanol | | 26.23 | 12.14 | 6.70 | | 2136 | 1:1 | $V_D$ |
| 2. | 2-methoxyethanol | $P_{212121}$ | 7.04 | 13.08 | 22.81 | 90 | 2100 | 1:1 | $IV_D$ |
| | ethyl acetate | | 6.98 | 12.87 | 22.66 | | 2040 | 1:1 | $IV_D$ |
| | dichloromethane | | 7.01 | 12.72 | 22.73 | | 2028 | 1:1 | $IV_D$ |
| | nitromethane | | 6.96 | 12.91 | 22.38 | | 2006 | 1:1 | $IV_D$ |
| | *n*- propanol | | 7.00 | 13.09 | 22.83 | | 2087 | 1:1 | $IV_D$ |
| | *n*- butanol | | 7.07 | 12.82 | 23.05 | | 2087 | 1:1 | $IV_D$ |
| | isopropanol | | 7.03 | 12.99 | 23.03 | | 2095 | 1:1 | $IV_D$ |
| | *n*- pentanol | | 7.02 | 12.93 | 22.95 | | 2084 | 1:1 | $IV_D$ |
| | cyclohexanol | | 7.04 | 12.73 | 22.83 | | 2088 | 1:1 | $IV_D$ |
| | tetrahydrofuran | | 7.02 | 12.98 | 23.14 | | 2109 | 1:1 | $IV_D$ |
| | 1,3-dioxolane | | 7.03 | 13.01 | 22.82 | | 2084 | 1:1 | $IV_D$ |
| | ethanol | | 6.96 | 12.98 | 22.63 | | 2047 | 1:1 | $IV_D$ |
| | methanol | | 6.98 | 13.10 | 22.58 | | 2068 | 1:1 | $IV_D$ |
| | acetone | | 6.98 | 13.00 | 22.70 | | 2063 | 1:1 | $IV_D$ |
| | pyridine | | 7.00 | 12.81 | 22.98 | | 2064 | 1:1 | $IV_D$ |
| | benzene | | 7.09 | 13.07 | 23.88 | | 2214 | 1:1 | $IV_D$ |
| 3. | dimethylacetamide | $P_{21}$ | 13.67 | 7.39 | 11.34 | 90.2 | 1110 | 1:1 | $IV_D$ |
| | N-methyl-2 pyrrolidone | | 13.92 | 7.35 | 11.39 | 90.3 | 1167 | 1:1 | $IV_D$ |
| | acetic acid | | 13.96 | 7.05 | 11.39 | 91.0 | 1119 | 1:2 | $VIII_D$/ $IX_D$ |
| | propionic acid | | 14.49 | 7.02 | 11.64 | 90.7 | 1185 | 1:2 | amorphous |
| Other | acetonitrile | $P_{21}$ | 13.33 | 7.55 | 10.45 | 112.3 | 972 | 1:1 | $IV_D$ /$VI_D$ |
| | acetonitrile (5 °C) | $P_{212121}$ | 9.33 | 34.97 | 6.81 | 90 | 2224 | 1:2 | $S_{ACN-II}$ |
| | acetonitrile [a] | $P_{212121}$ | 9.47 | 29.42 | 6.99 | 90 | 1945 | 1:1 | $IV_D$ /$XII_D$ |
| | formic acid | $P_{21}$ | 14.21 | 7.05 | 12.38 | 114.5 | 1132 | 1:2 | $S_{FA}$ |
| | formic acid [a] | $P_{212121}$ | 28.50 | 19.06 | 6.98 | 90 | 3797 | 1:1 | $VII_D$/$XI_D$ |
| | p-xylene | $P_{21}$ | 17.09 | 7.28 | 17.54 | 90.2 | 2206 | 1:0.5 | $IV_D$ |
| | cyclohexanol | $P_{21}$ | 13.92 | 12.07 | 6.84 | 90.8 | 1153 | 1:1 | $IV_D$ |
| | benzyl alcohol | $P_{212121}$ | 18.87 | 17.76 | 7.02 | 90 | 2352 | 1:1 | $IV_D$ |

[a] obtained in solid state transition from higher solvate

## SI 2. Thermal Characterization and VT-PXRD.

**Table S2.** Thermal data (DSC, TGA) for the Enc-HCl solvates

| | guest loss ($T_{peak}$), °C | weight loss, % | stoichiometry | thermal desolvation product |
|---|---|---|---|---|
| $S_{IBA}$ | 138 | 16.5 | 1:1 | $V_D$ |
| $DS_{ACN}$ | 79 | 18.5 | 2:1 | $IV_D$ |
| $S_{ACN-I}$ | 84 | 9.8 | 1:1 | $IV_D$ |
| $S_{ACN-II}$ | 72 | 10.6 | 1:1 | $IV_D$ |
| $S_{FA}$ | 120 | 11.5 | 1:1 | $VII_D$ |
| $DS_{FA}$ | 60; 120 | 24.0 | 2:1 | $S_{FA}$/ $VII_D$ |
| $DS_{AA}$ | 115 | 21.6 | 2:1 | IXD |
| $S_{BnOH}$ | 123 | 24.9 | 1:1 | $IV_D$ |
| $S_{EtOH}$ | 99 | 11.2 | 1:1 | $IV_D$ |

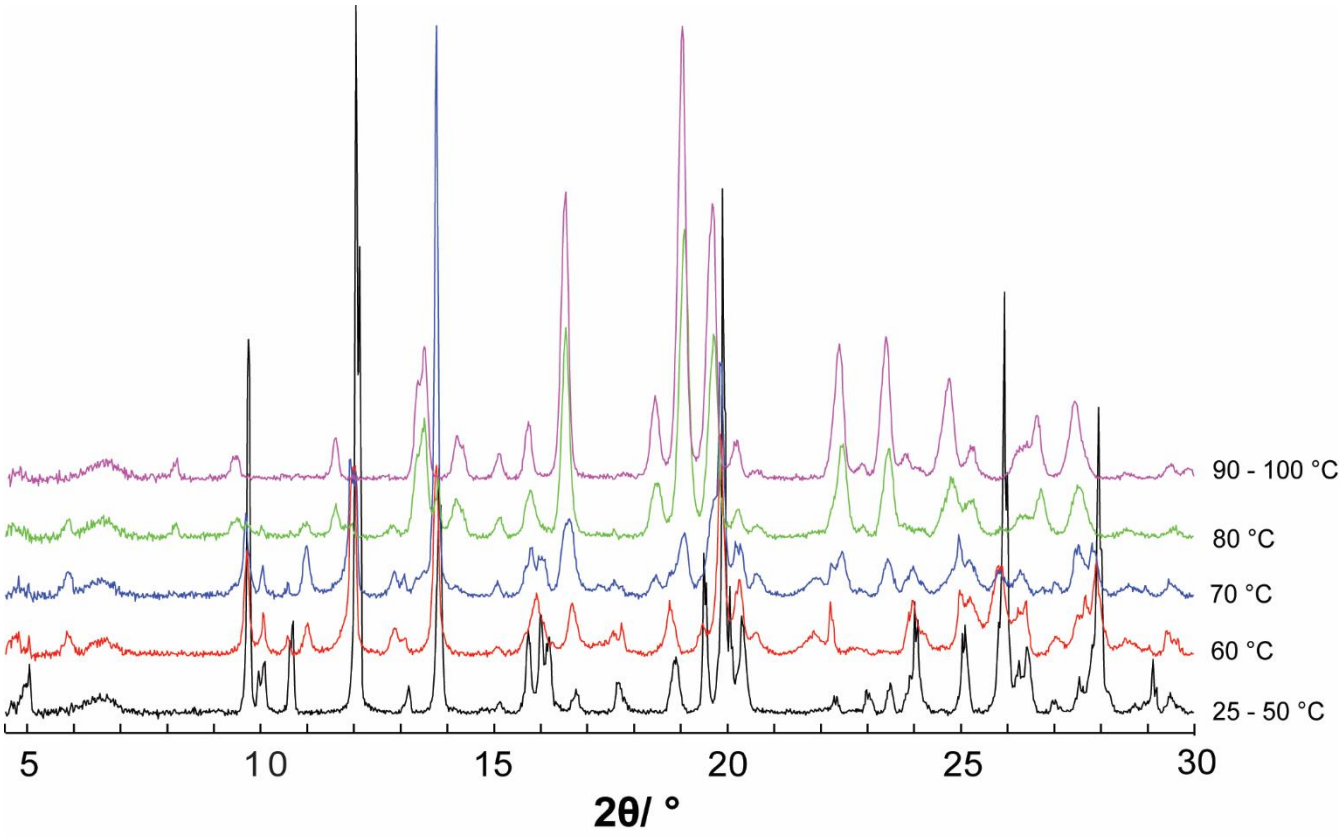


**Figure S1.** VT-PXRD patterns of Enc-HCl acetonitrile disolvate- $DS_{ACN}$.

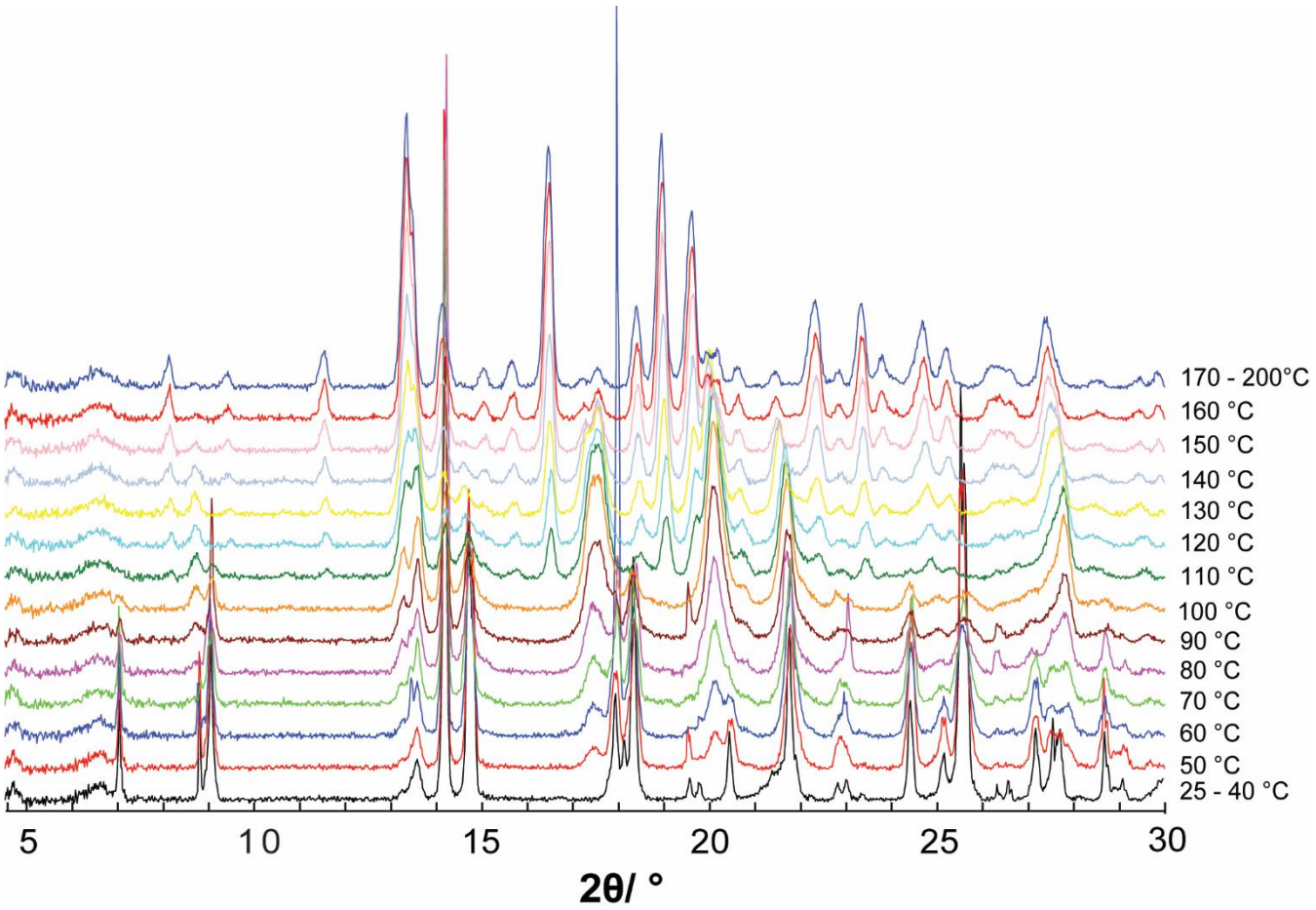


**Figure S2.** VT-PXRD patterns of Enc-HCl acetonitrile monosolvate- $S_{ACN-I}$.

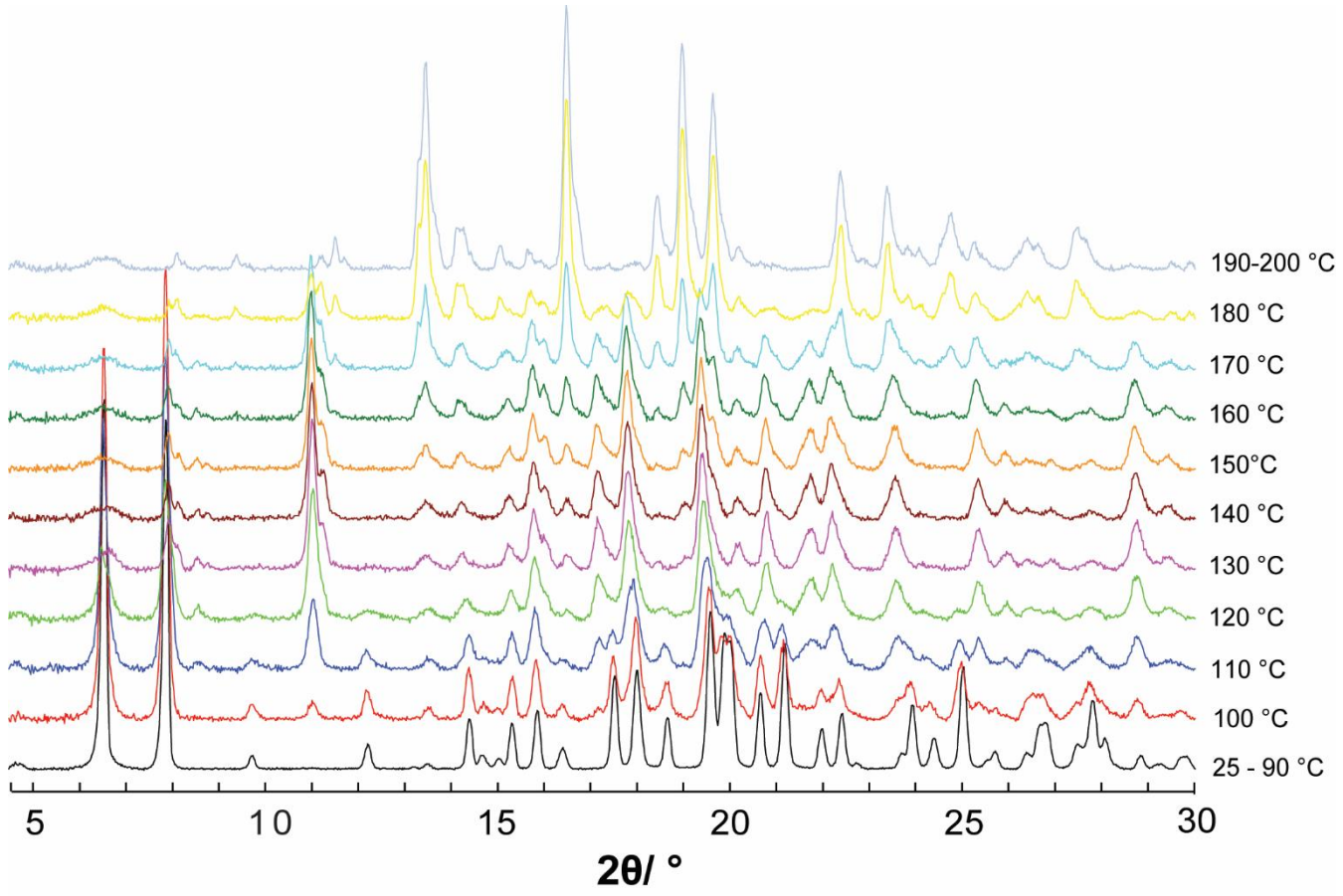


**Figure S3.** VT-PXRD patterns of Enc-HCl isobutanol monosolvate- $S_{IBA}$.

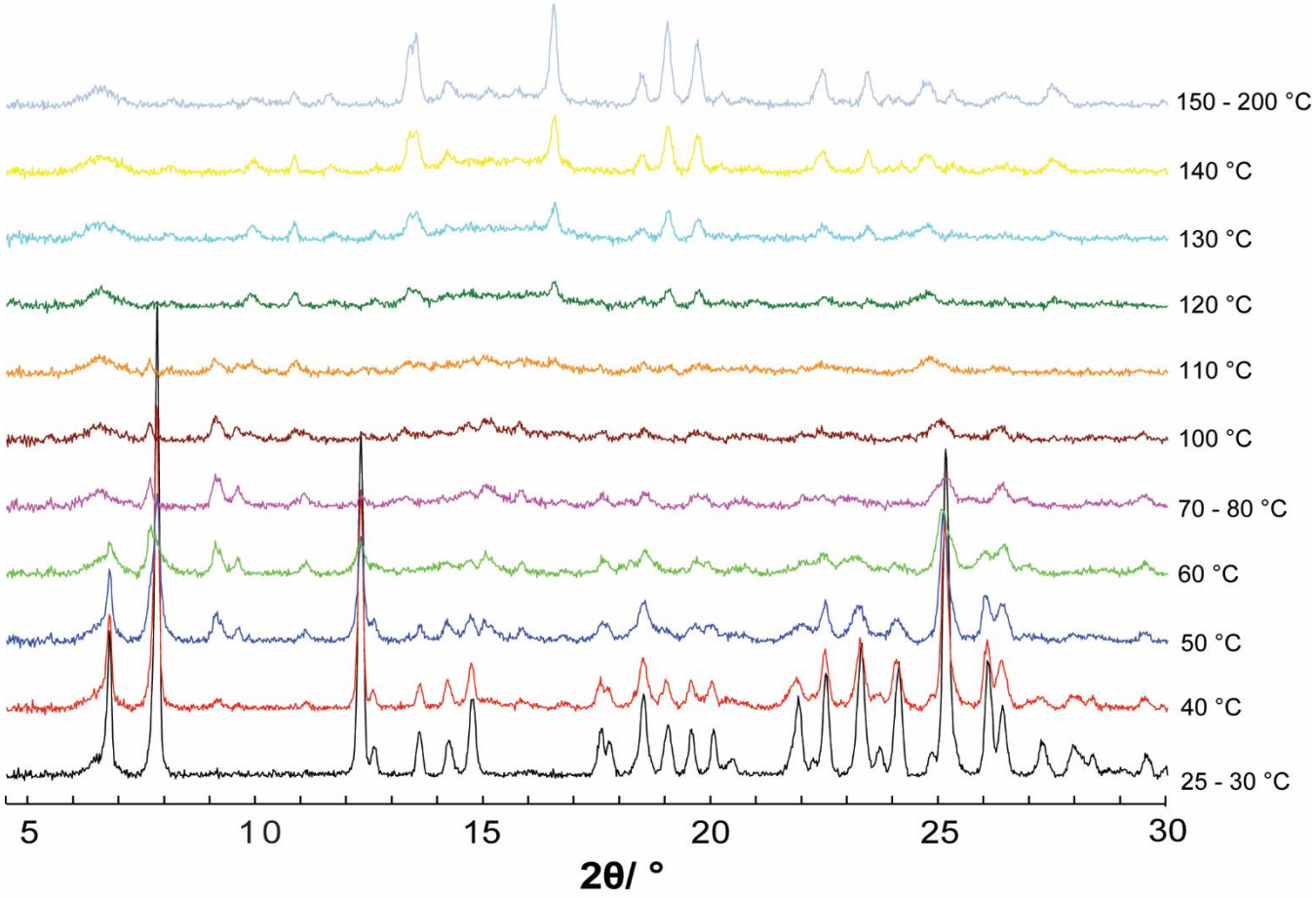


**Figure S4.** VT-PXRD patterns of Enc-HCl formic acid disolvate- $DS_{FA}$.

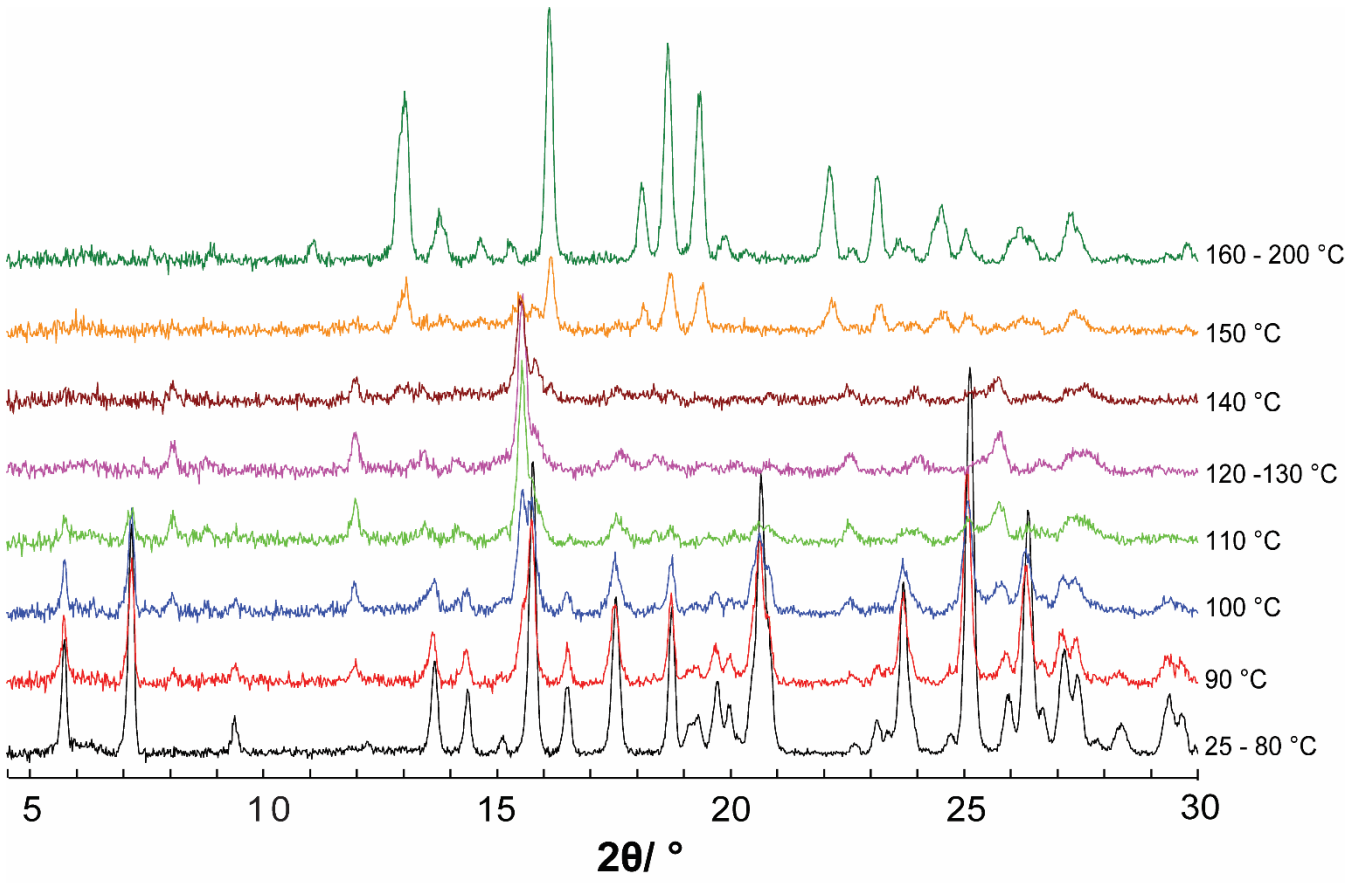


**Figure S5.** VT-PXRD patterns of Enc-HCl acetic acid disolvate- $DS_{AA}$.

### 3. Monohydrate MH-V and MH-VI characterization

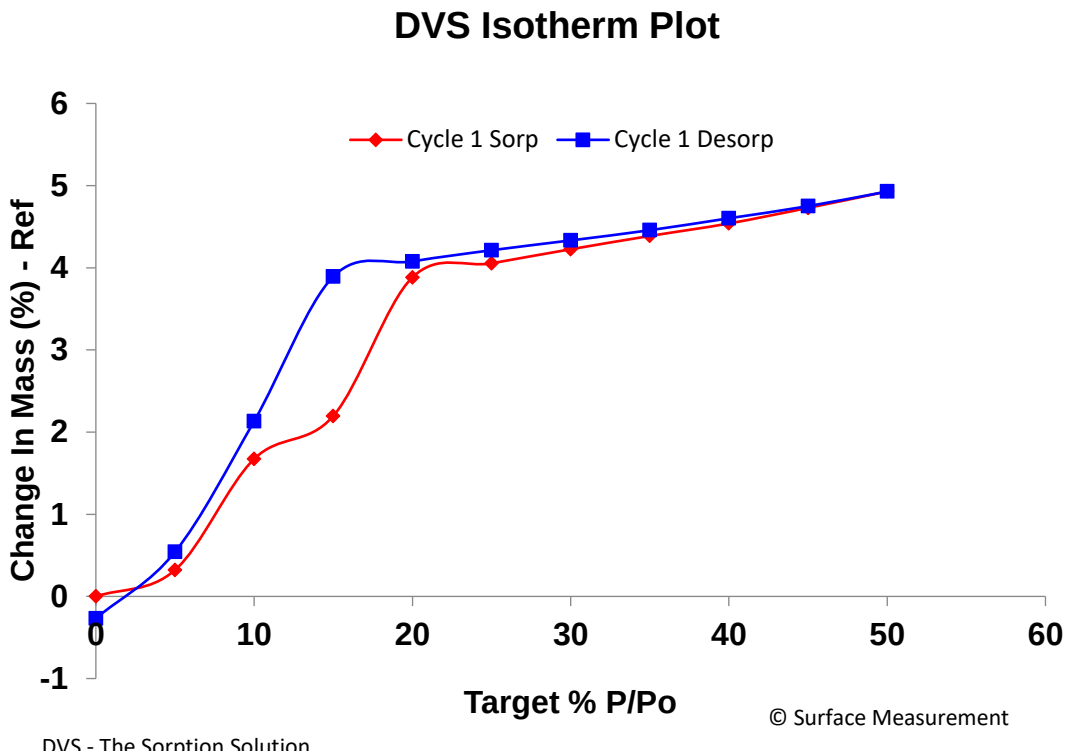


**Figure S6.** DVS isotherms of Enc-HCl monohydrate MH-V at 25 °C.

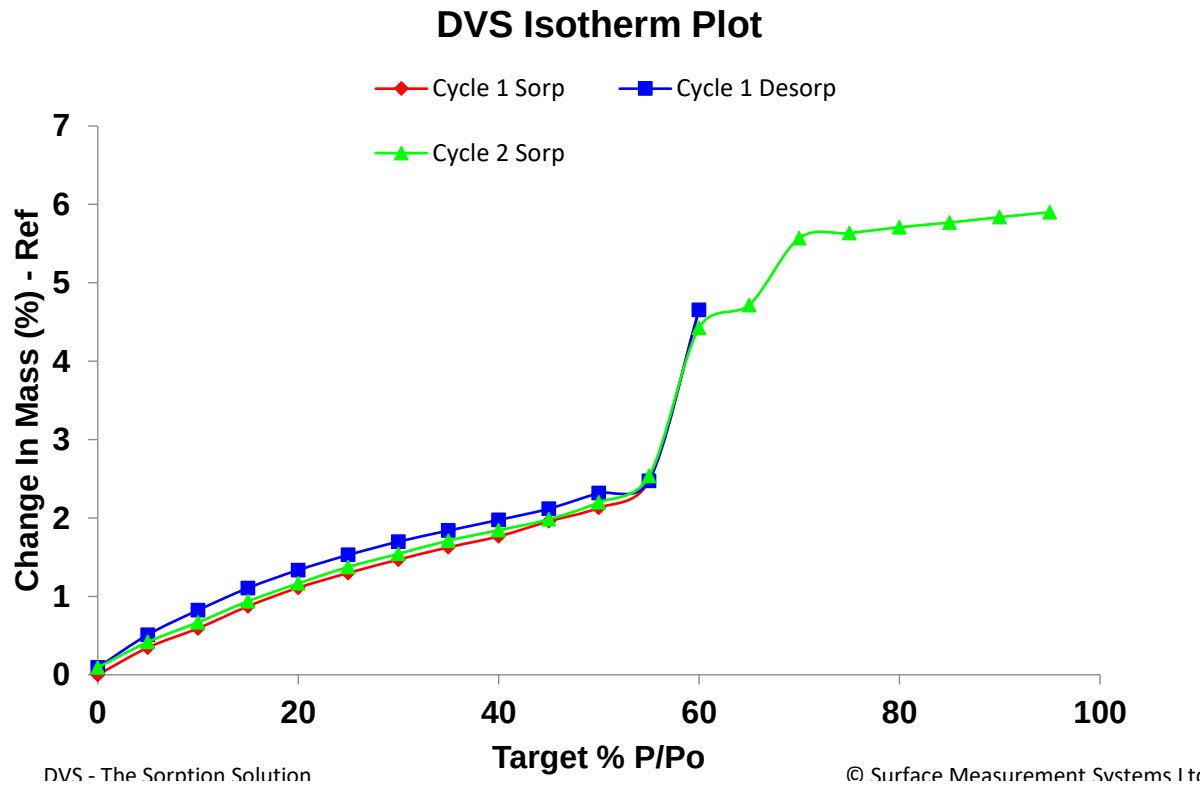


**Figure S7.** DVS isotherms of Enc-HCl monohydrate MH-VI at 25 °C.

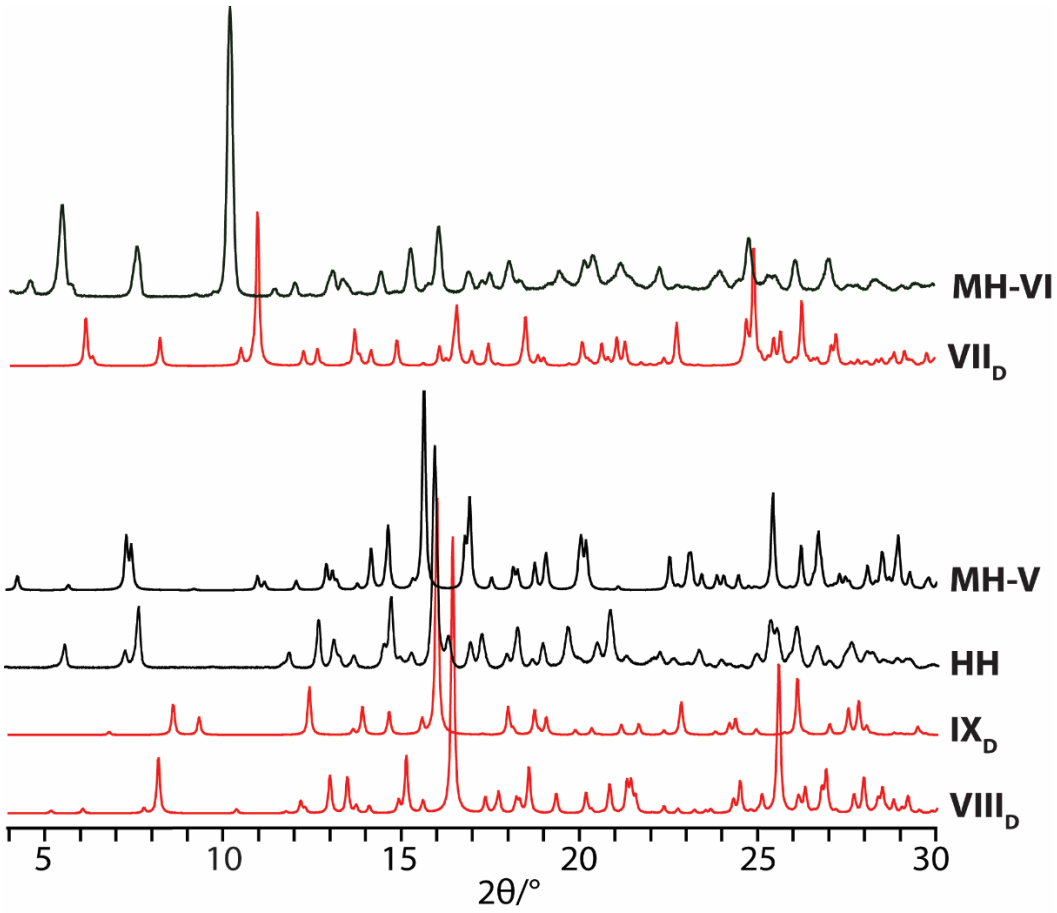


**Figure S8.** PXRD patterns of Enc-HCl nonsolvated (red) crystalline forms and their respective hydrated phases (black).

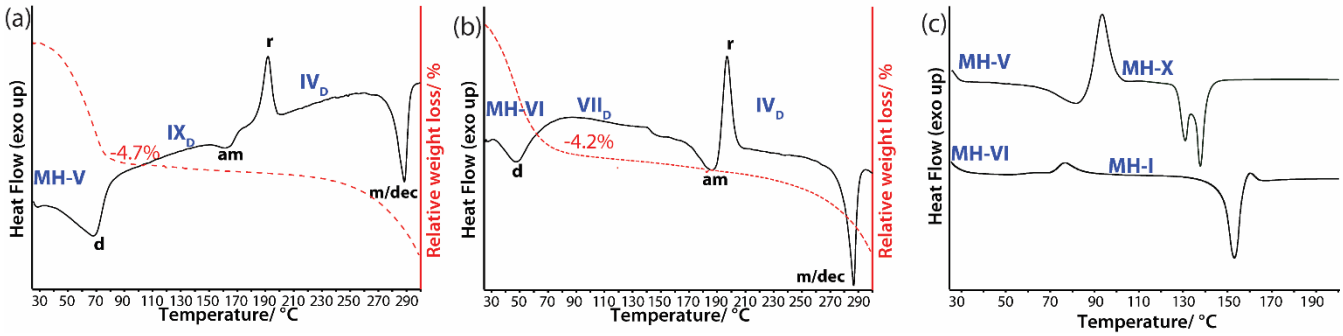


**Figure S9.** (a-b) DSC/TG traces of Enc-HCl monohydrates. d – desolvation, am – amorphization, r – recrystallization, m/dec – melting with decomposition (10 °C/min heating rate) in open crucibles. (c) Overlay of DSC curves of Enc-HCl monohydrates at 10 °C/min heating rate in sealed crucibles.

## SI 4. Crystal structure determination

**Table S3.** Crystal data for Enc-HCl solvated phases

| | **$DS_{AA}$** | **$S_{EtOH}$** | **$DS_{ACN}$** | **$S_{ACN-I}$** | **$S_{ACN-II}$** | **$S_{IBA}$** | **$S_{FA}$** | **$S_{BnOH}$** | **MH-V** |
|---|---|---|---|---|---|---|---|---|---|
| formula | $C_{20}H_{26}Cl_2N_2O_5S$ | $C_{18}H_{23}Cl_2N_2O_2S$ | $C_{20}H_{24}Cl_2N_4OS$ | $C_{18}H_{21}Cl_2N_3OS$ | $C_{18}H_{21}Cl_2N_3OS$ | $C_{20}H_{28}Cl_2N_2O_2S$ | $C_{17}H_{20}Cl_2N_2O_3S$ | $C_{23}H_{26}Cl_2N_2O_2S$ | $C_{16}H_{20}Cl_2N_2O_2S$ |
| formula weight, $g \cdot mol^{-1}$ | 477.39 | 403.35 | 439.39 | 398.34 | 398.34 | 431.40 | 403.31 | 465.42 | 375.30 |
| sample type | crystal | crystal | crystal | crystal | powder | powder | powder | powder | powder |
| crystal system | monoclinic | orthorhombic | orthorhombic | monoclinic | orthorhombic | orthorhombic | orthorhombic | orthorhombic | monoclinic |
| space group | $P2_1$ | $P2_12_12_1$ | $P2_12_12_1$ | $P2_1$ | $P2_12_12_1$ | $P2_12_12_1$ | $P2_12_12_1$ | $P2_12_12_1$ | $P2_1$ |
| a, Å | 13.8812(4) | 6.9170(2) | 6.6818(2) | 10.25590(10) | 29.424(3) | 26.533(16) | 28.5929(10) | 18.8294(7) | 18.3333(8 |
| b, Å | 6.8563(2) | 13.0268(5) | 9.2833(2) | 7.50830(10) | 9.4777(10) | 12.1649(8) | 19.1266(8) | 17.7219(7) | 6.98761(17) |
| c, Å | 11.4582(4) | 21.8980(8) | 35.0845(5) | 13.3761(2) | 6.9991(7 | 6.6952(4) | 7.0043(2) | 7.0016(3) | 14.2176(5) |
| α, ° | 90 | 90 | 90 | 90 | 90 | 90 | 90 | 90 | 90 |
| β, ° | 90.293(3) | 90 | 90 | 112.478(2) | 90 | 90 | 90 | 90 | 91.052(2) |
| γ, ° | 90 | 90 | 90 | 90 | 90 | 90 | 90 | 90 | 90 |
| V, $Å^3$ | 1090.51(6) | 1973.15(12) | 2176.26(9) | 951.76(2) | 1951.9(3) | 2161.0(13) | 3830.6(2) | 2336.38(16) | 1821.05(11 |
| $\rho_{calc}$, $g \cdot cm^{-3}$ | 1.45 | 1.36 | 1.34 | 1.39 | 1.36 | 1.33 | 1.40 | 1.32 | 1.37 |
| Z/ Z' | 2/1 | 4/1 | 4/1 | 2/1 | 4/1 | 4/1 | 8/2 | 4/1 | 4/2 |
| temperature, K | 174 | 174 | 174 | 150 | 293 | 293 | 293 | 293 | 293 |
| $2\theta_{min}$–$2\theta_{max}$ /increment, ° | - | - | - | - | 4.5–70/0.01 | 4.5–70/0.01 | 5.0-70/0.005 | 4.0–70/0.01 | 4.0–70/0.01 |
| *Rwp* | - | - | - | - | 0.04911 | 0.03790 | 0.05833 | 0.04829 | 0.02597 |
| *Rp* | - | - | - | - | 0.07324 | 0.02917 | 0.04338 | 0.03661 | 0.03695 |
| $R_{exp}$ | - | - | - | - | 0.04460 | 0.01124 | 0.05465 | 0.01239 | 0.00641 |
| $R_1$ ($wR_2$) | 0.0406 (0.0510) | 0.0335 (0.0398) | 0.0303 (0.0368) | 0.0255 (0.0680) | - | | - | | |
| Packing index, % [a] | 73.5 | 72.1 | 73.3 | 73.6 | 72.2 | 72.8 | 72.2 | 72.0 | 68.2 |
| CCDC no. | 1895195 | 1895190 | 1916268 | 1916267 | 1916269 | 1895198 | 1895189 | 1895191 | 1916266 |

[a] after geometry optimization by relaxing positions of all atoms and unit cell parameters

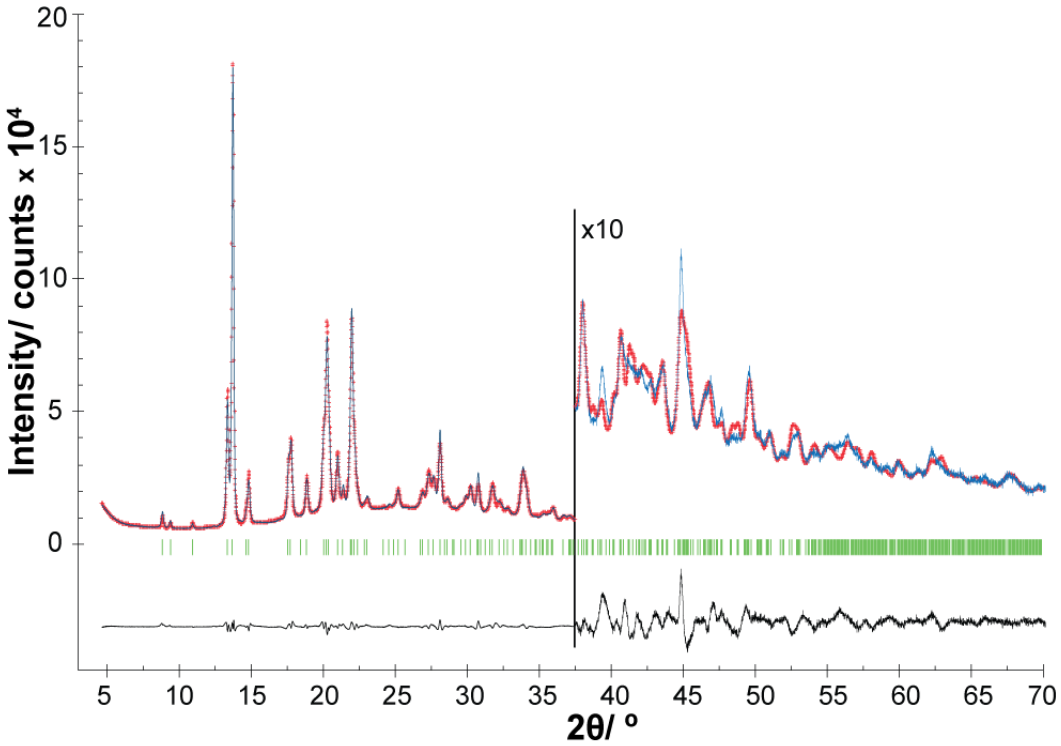


**Figure S10.** Final Rietveld fit for Enc-HCl polymorph $VI_D$: red crosses – measured data points; blue line – calculated profile; black line – difference curve; green tick marks – calculated peak positions.

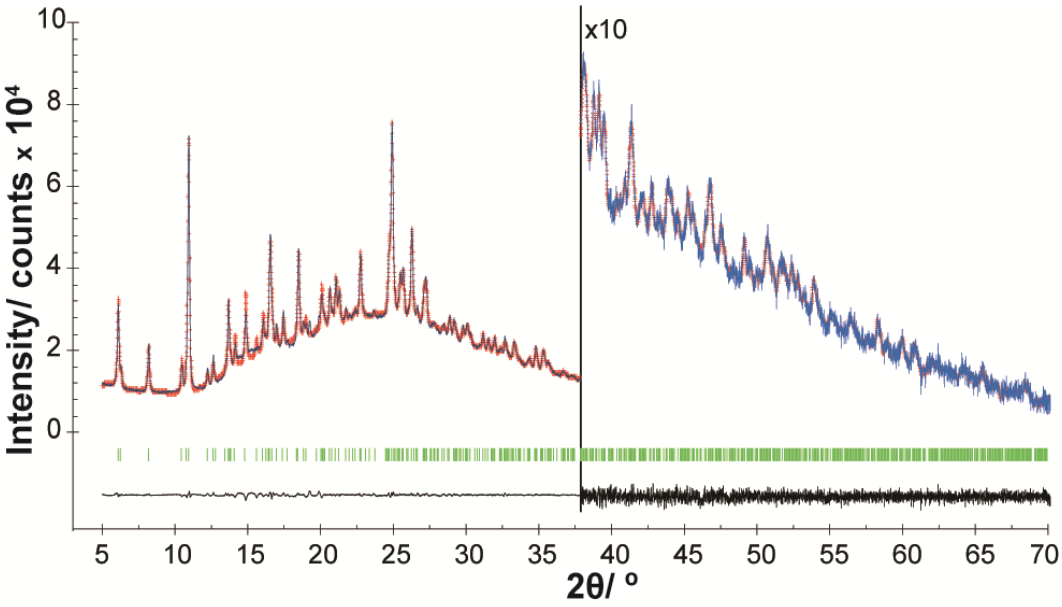


**Figure S11.** Final Rietveld fit for Enc-HCl polymorph $VII_D$: red crosses – measured data points; blue line – calculated profile; black line – difference curve; green tick marks – calculated peak positions.

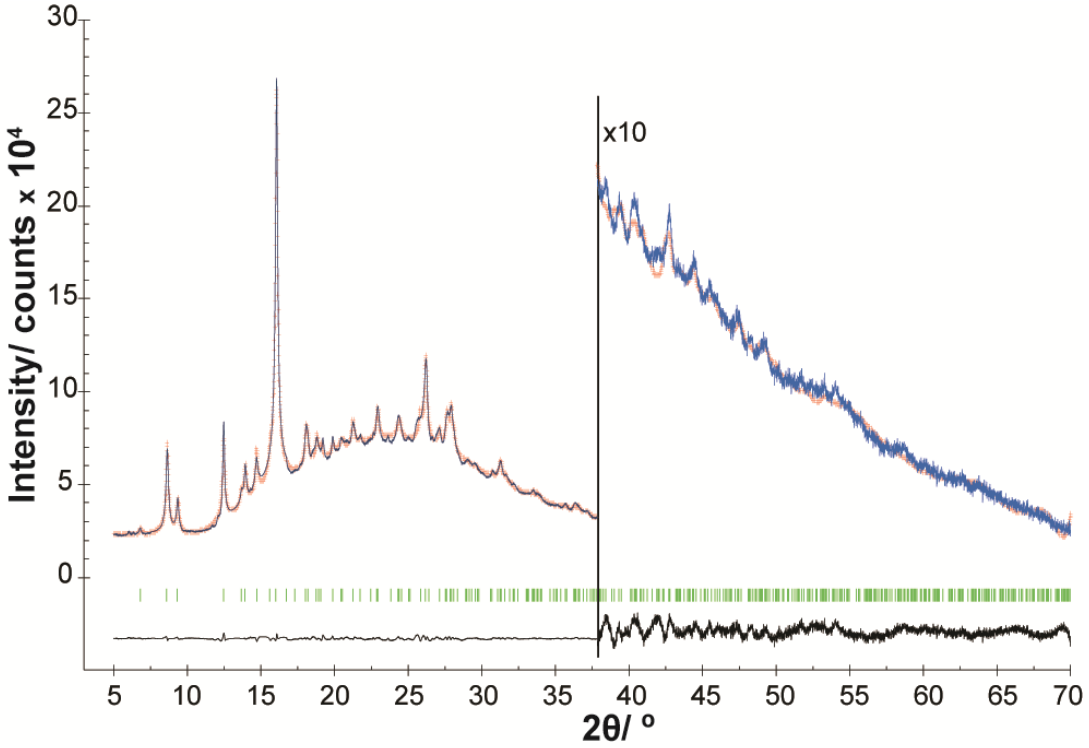


**Figure S12.** Final Rietveld fit for Enc-HCl polymorph $VIII_D$: red crosses – measured data points; blue line – calculated profile; black line – difference curve; green tick marks – calculated peak positions.

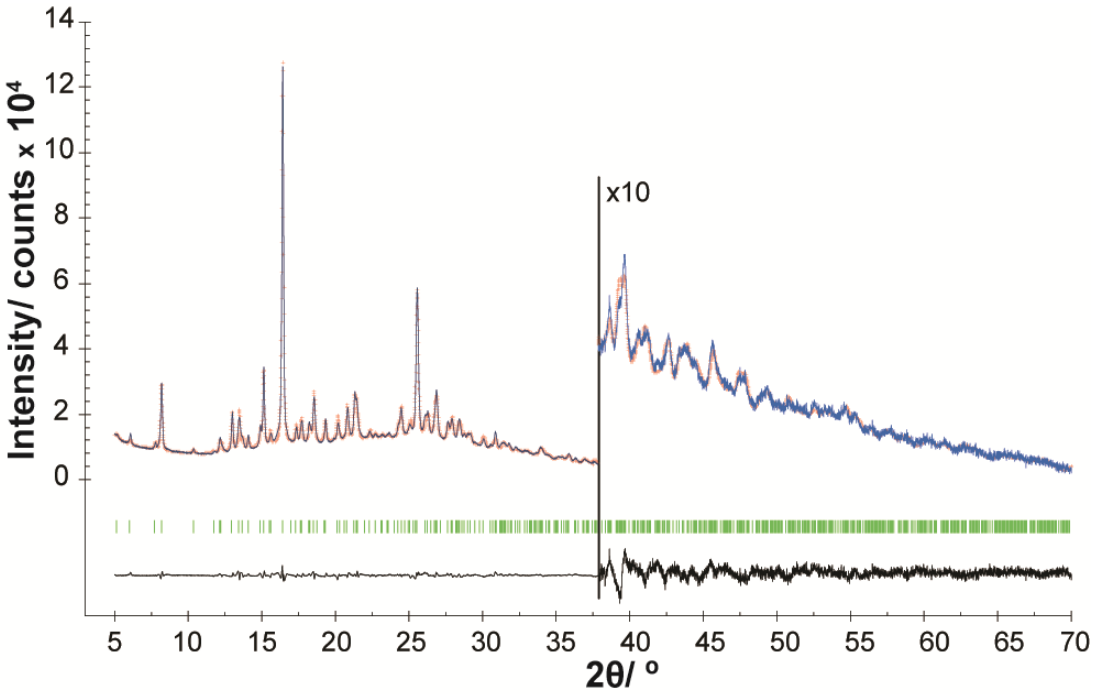


**Figure S13.** Final Rietveld fit for Enc-HCl polymorph $IX_D$: red crosses – measured data points; blue line – calculated profile; black line – difference curve; green tick marks – calculated peak positions.

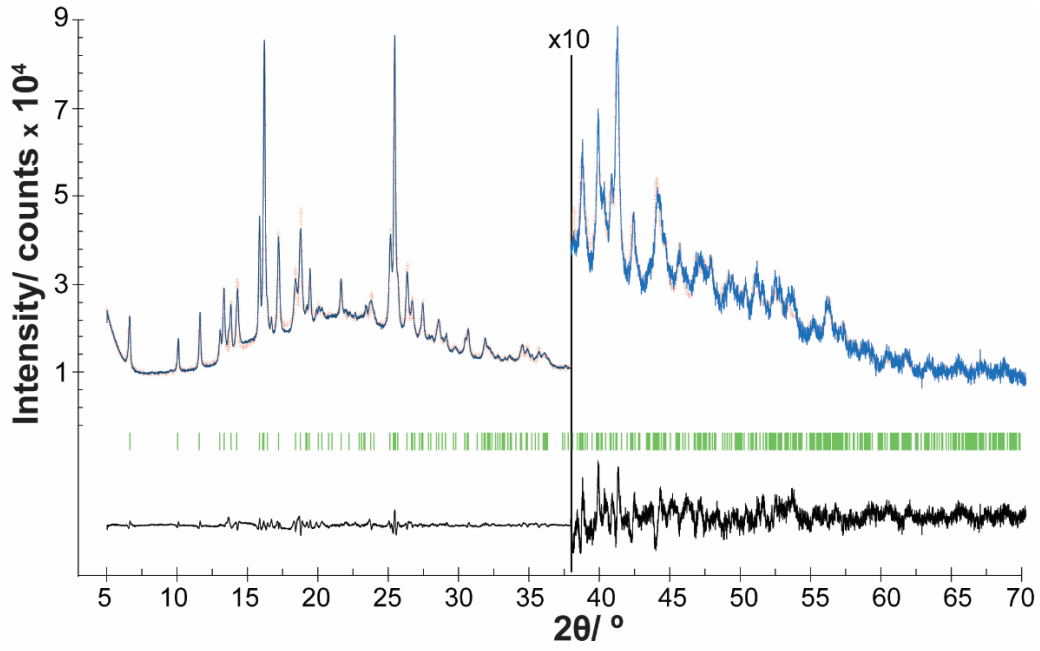


**Figure S14.** Final Rietveld fit for Enc-HCl polymorph $XII_D$: red crosses – measured data points; blue line – calculated profile; black line – difference curve; green tick marks – calculated peak positions.

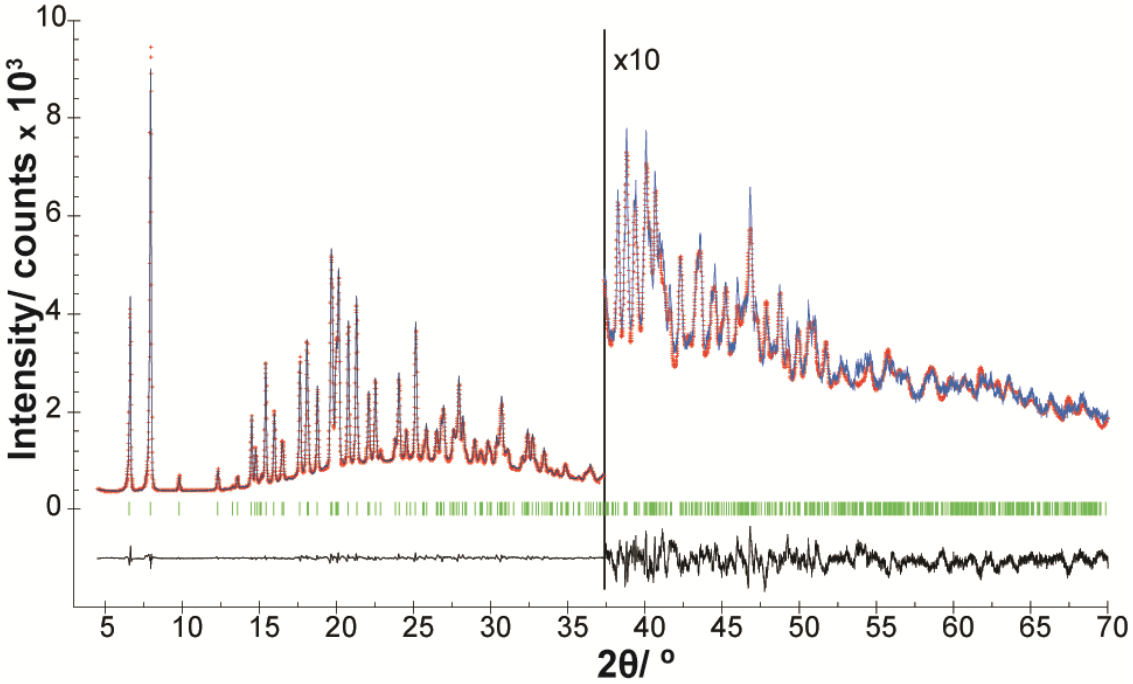


**Figure S15.** Final Rietveld fit for Enc-HCl i-butanol monosolvate $S_{IBA}$: red crosses – measured data points; blue line – calculated profile; black line – difference curve; green tick marks – calculated peak positions.

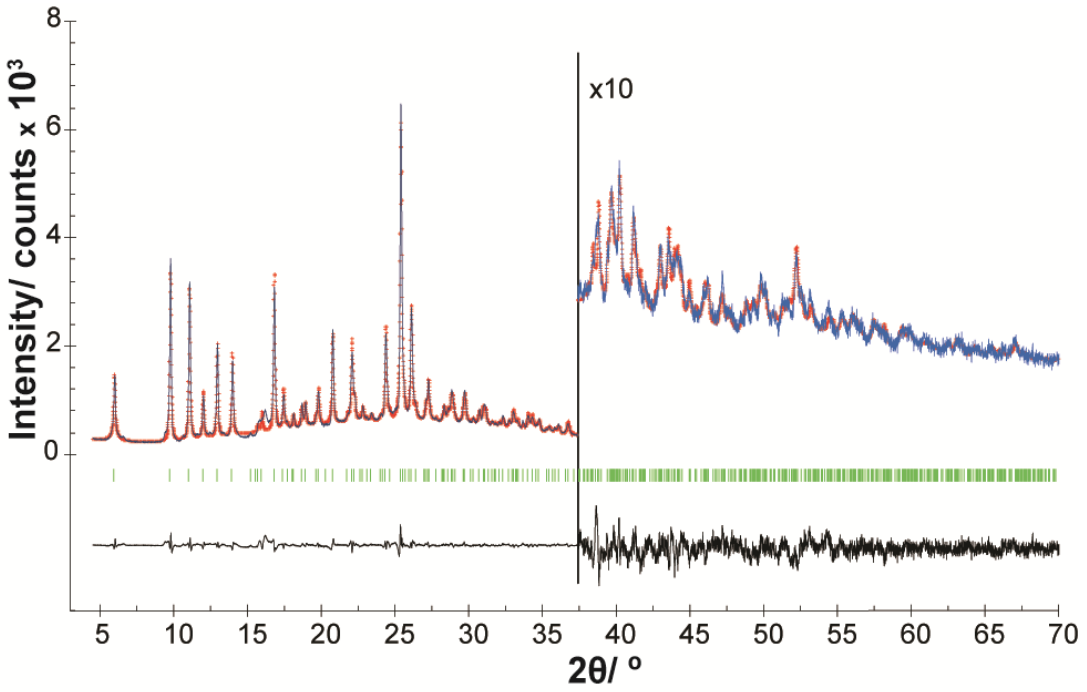


**Figure S16.** Final Rietveld fit for Enc-HCl acetonitrile monosolvate I $S_{ACN-II}$: red crosses – measured data points; blue line – calculated profile; black line – difference curve; green tick marks – calculated peak positions.

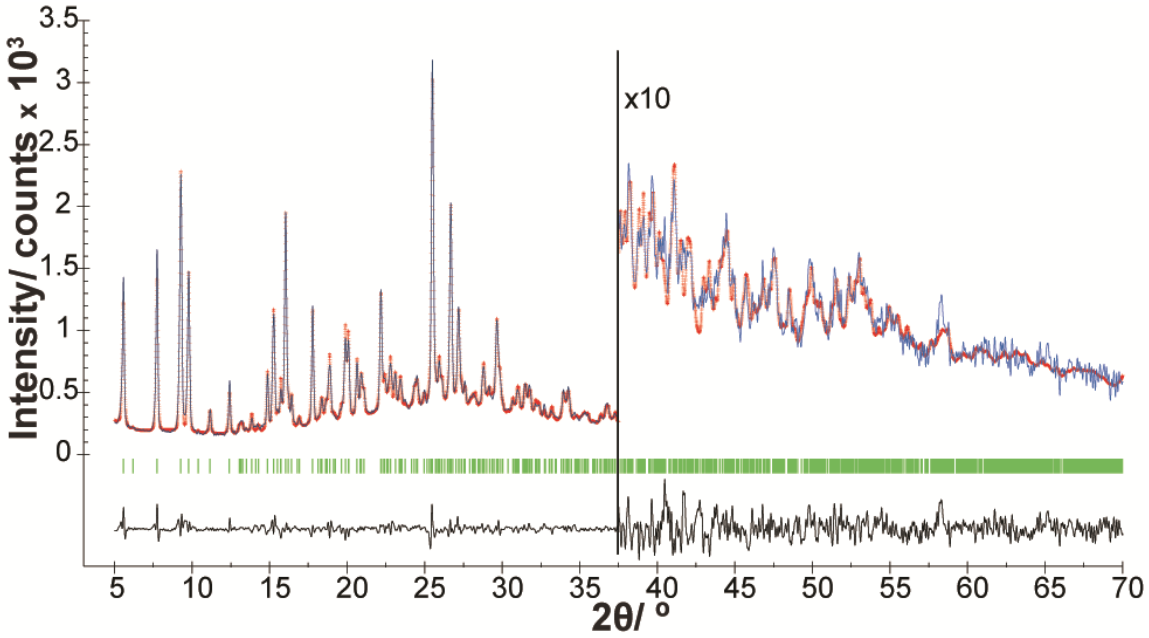


**Figure S17.** Final Rietveld fit for Enc-HCl formic acid monosolvate $S_{FA}$: red crosses – measured data points; blue line – calculated profile; black line – difference curve; green tick marks – calculated peak positions.

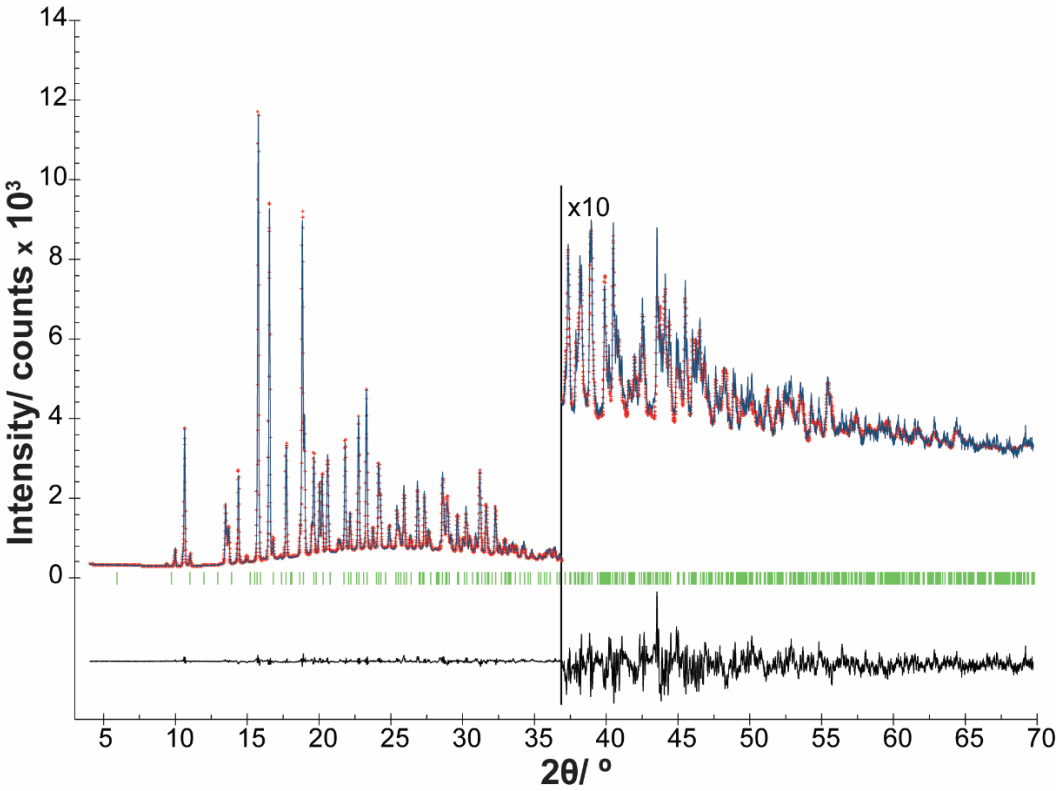


**Figure S18.** Final Rietveld fit for Enc-HCl benzyl alcohol monosolvate $S_{BnOH}$: red crosses – measured data points; blue line – calculated profile; black line – difference curve; green tick marks – calculated peak positions.

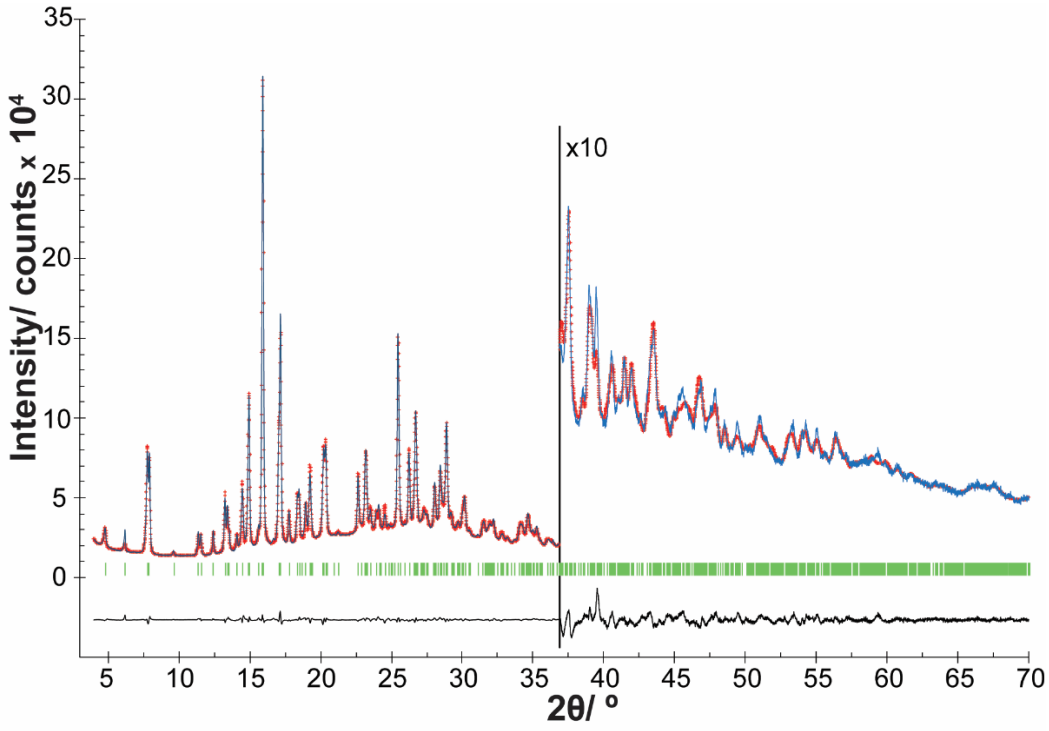


**Figure S19.** Final Rietveld fit for Enc-HCl monohydrate MH-V: red crosses – measured data points; blue line – calculated profile; black line – difference curve; green tick marks – calculated peak positions.

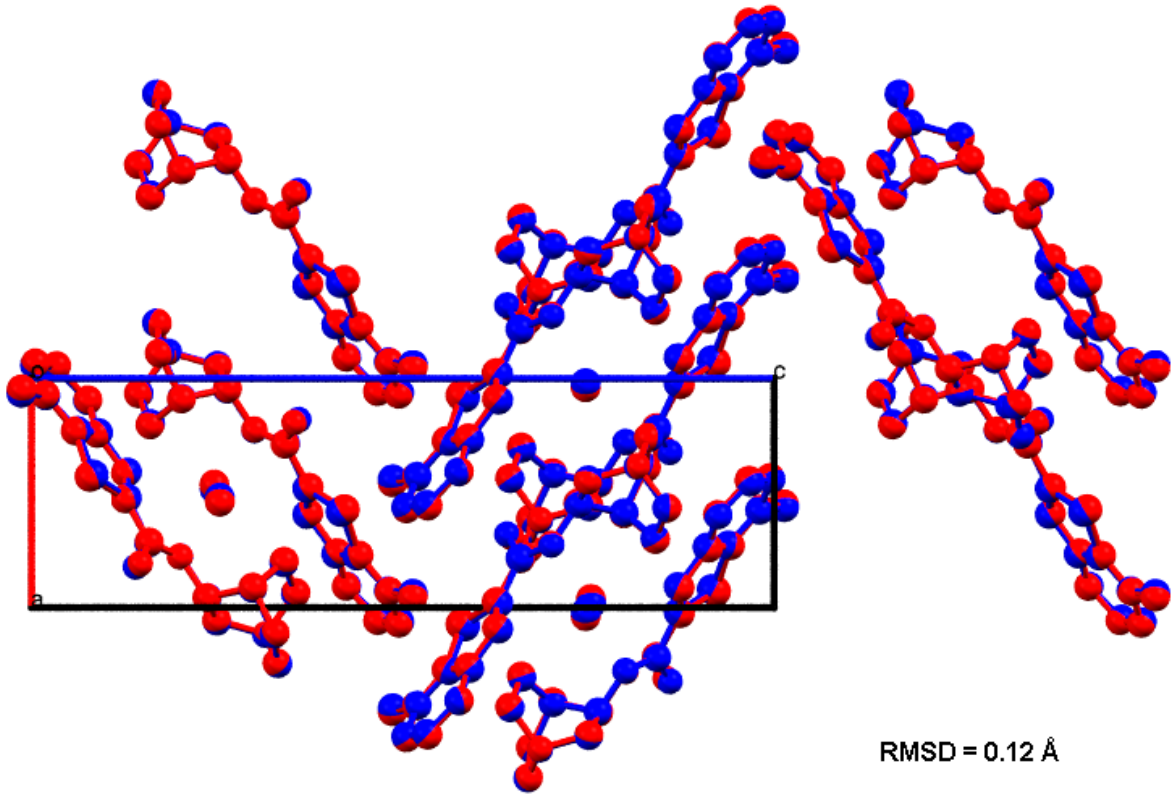


**Figure S20**. Overlay of form $V_D$ crystal structure calculated from PXRD data (blue) and crystal structure after DFT optimisation (red) with given $RMSD_{15}$ value for non-hydrogen atoms.

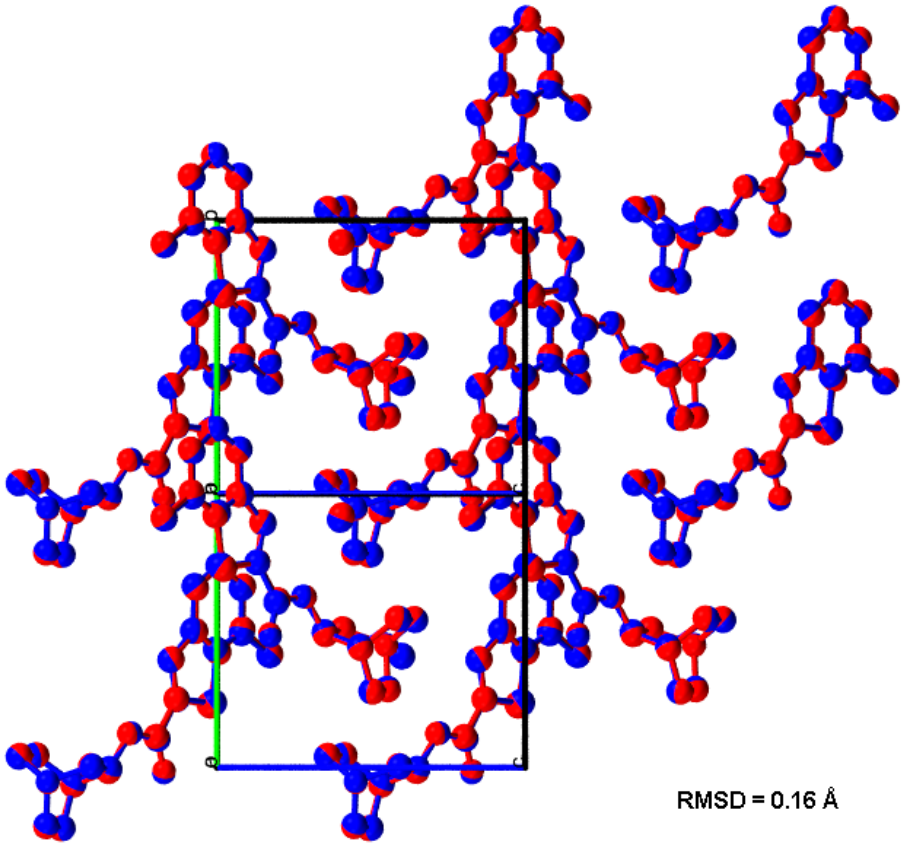


**Figure S21.** Overlay of form $VI_D$ crystal structure calculated from PXRD data (blue) and crystal structure after DFT optimisation (red) with given $RMSD_{15}$ value for non-hydrogen atoms.

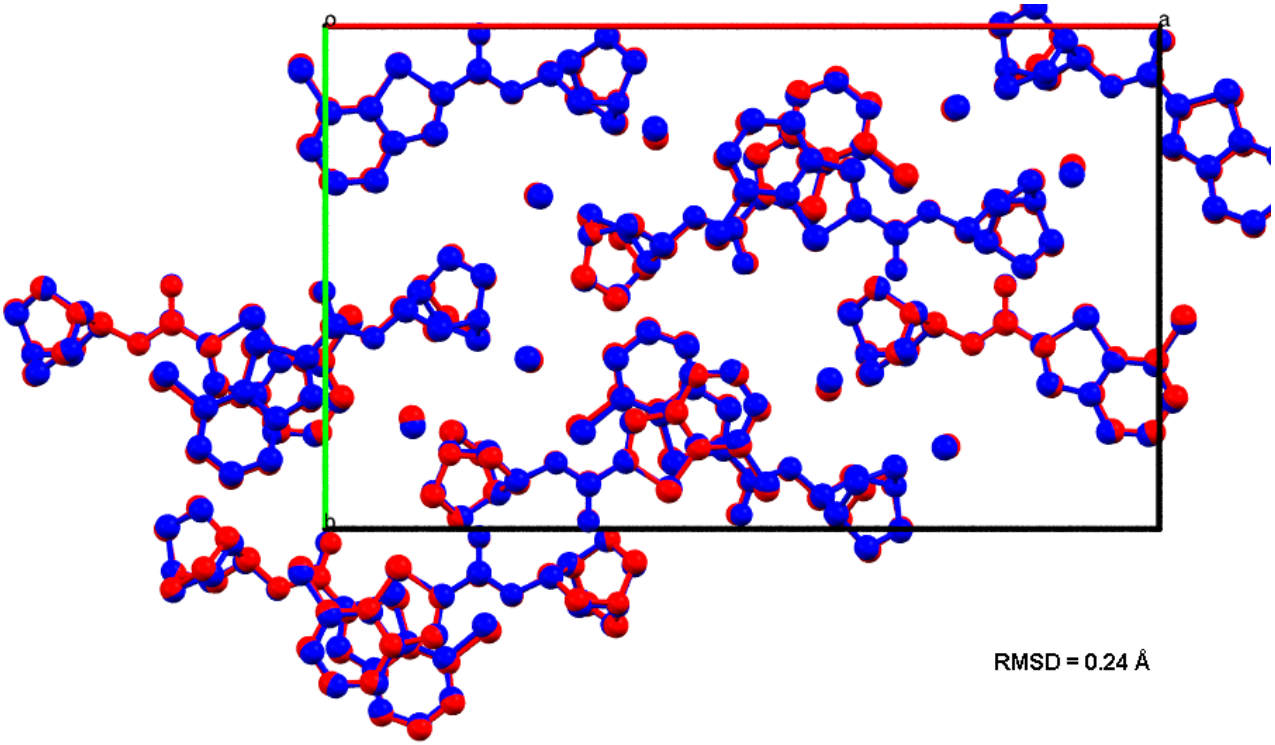


**Figure S22.** Overlay of form $VII_D$ crystal structure calculated from PXRD data (blue) and crystal structure after DFT optimisation (red) with given $RMSD_{15}$ value for non-hydrogen atoms.

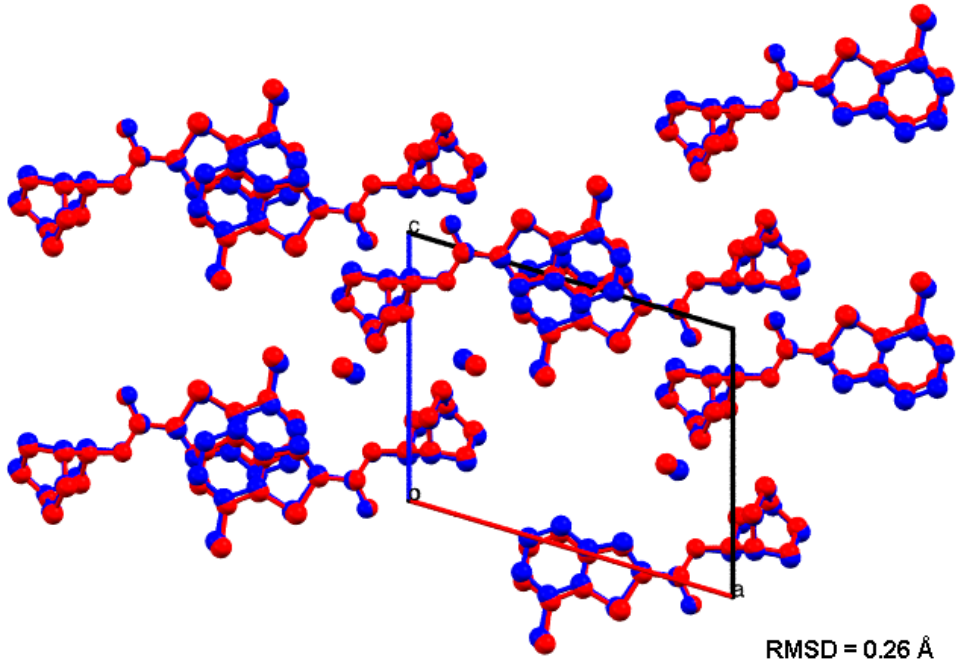


**Figure S23.** Overlay of form $VIII_D$ crystal structure calculated from PXRD data (blue) and crystal structure after DFT optimisation (red) with given $RMSD_{15}$ value for non-hydrogen atoms.

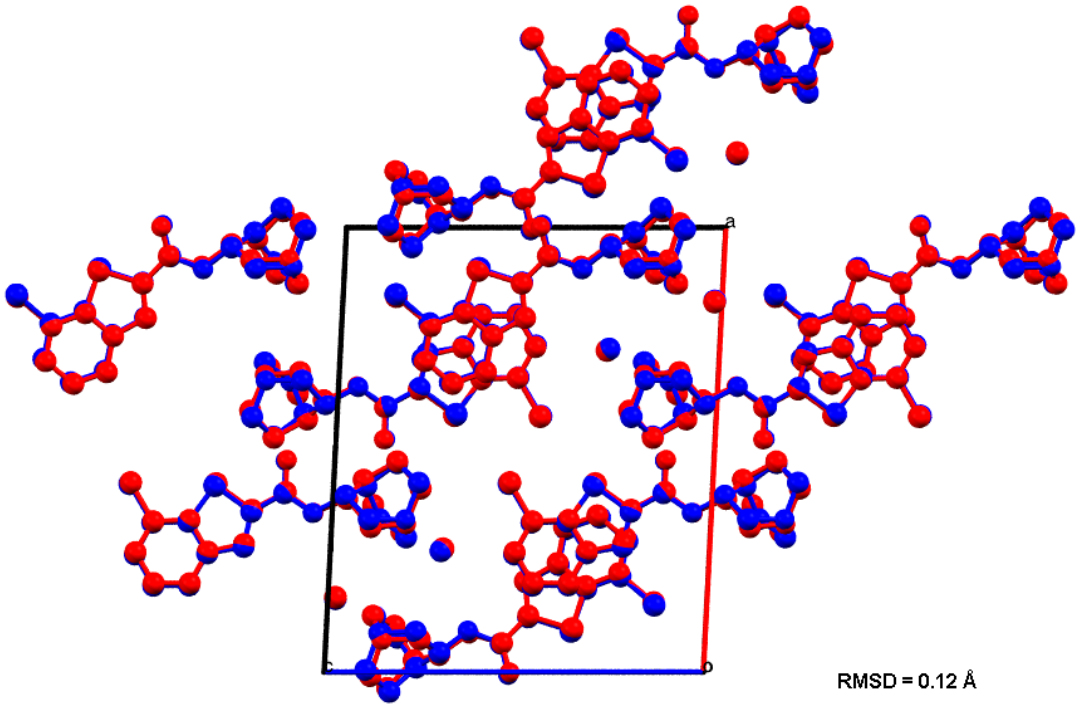


**Figure S24.** Overlay of form $IX_D$ crystal structure calculated from PXRD data (blue) and crystal structure after DFT optimisation (red) with given $RMSD_{15}$ value for non-hydrogen atoms.

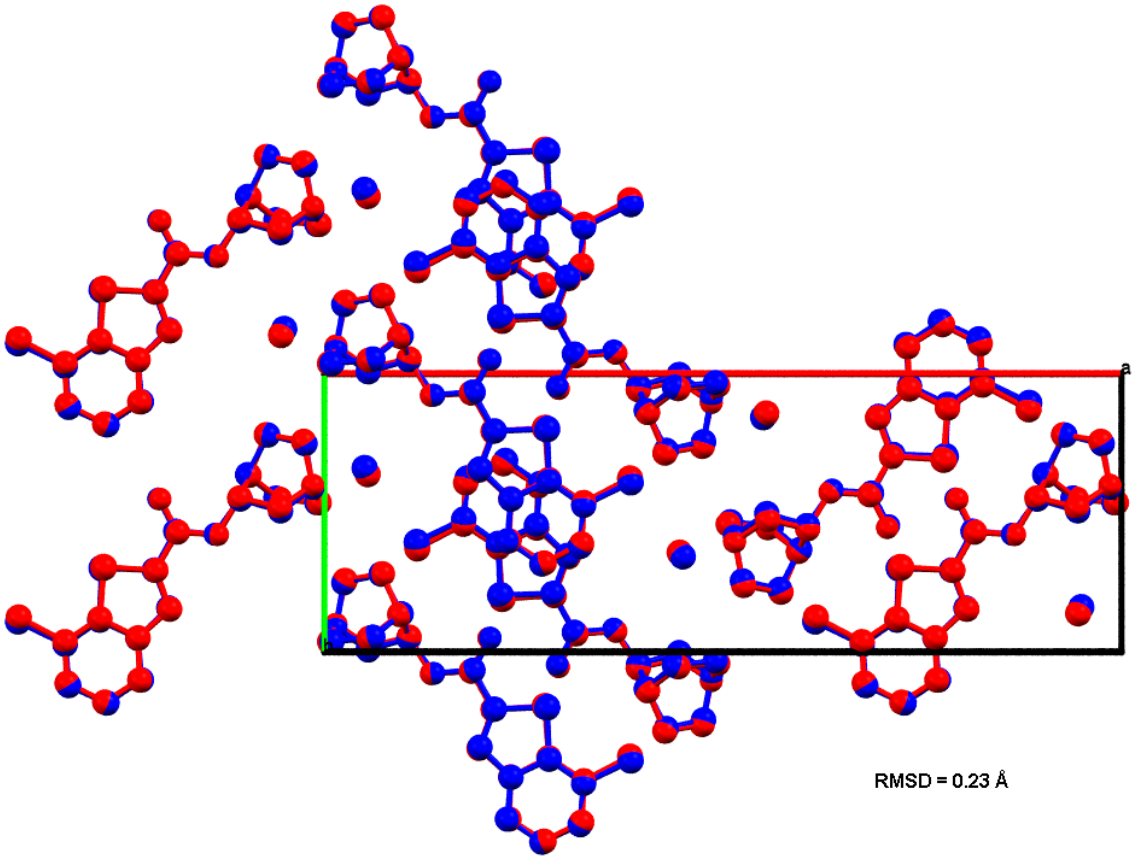


**Figure S25.** Overlay of form $XII_D$ crystal structure calculated from PXRD data (blue) and crystal structure after DFT optimisation (red) with given $RMSD_{15}$ value for non-hydrogen atoms.

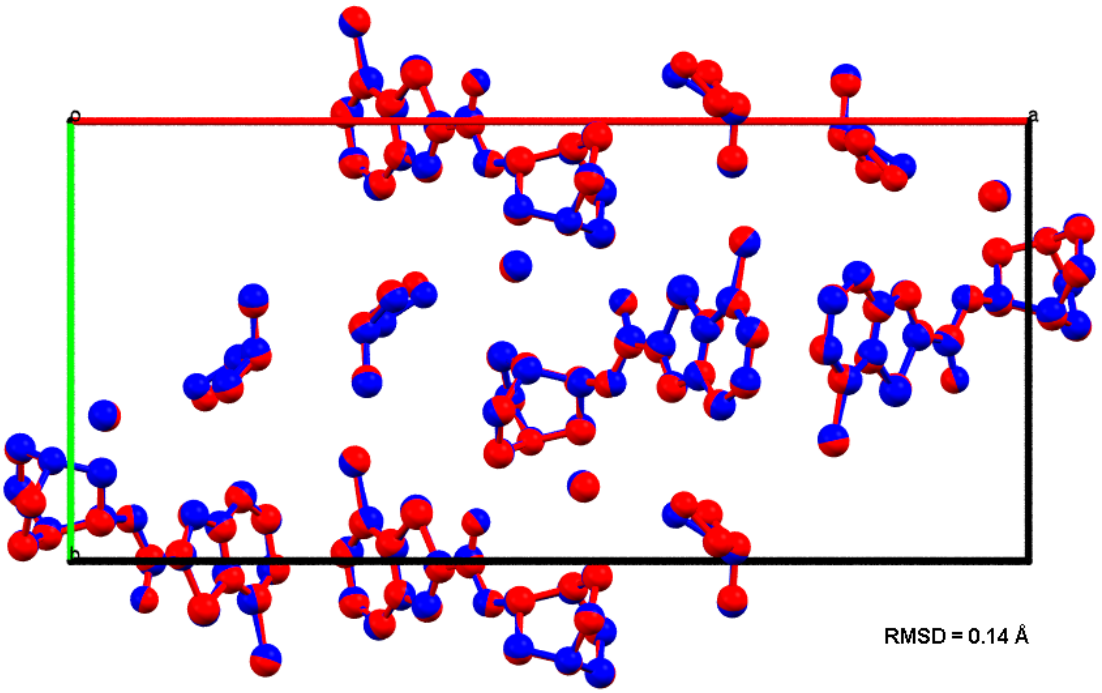


**Figure S26.** Overlay of form $S_{IBA}$ crystal structure calculated from PXRD data (blue) and crystal structure after DFT optimisation (red) with given $RMSD_{15}$ value for non-hydrogen atoms.

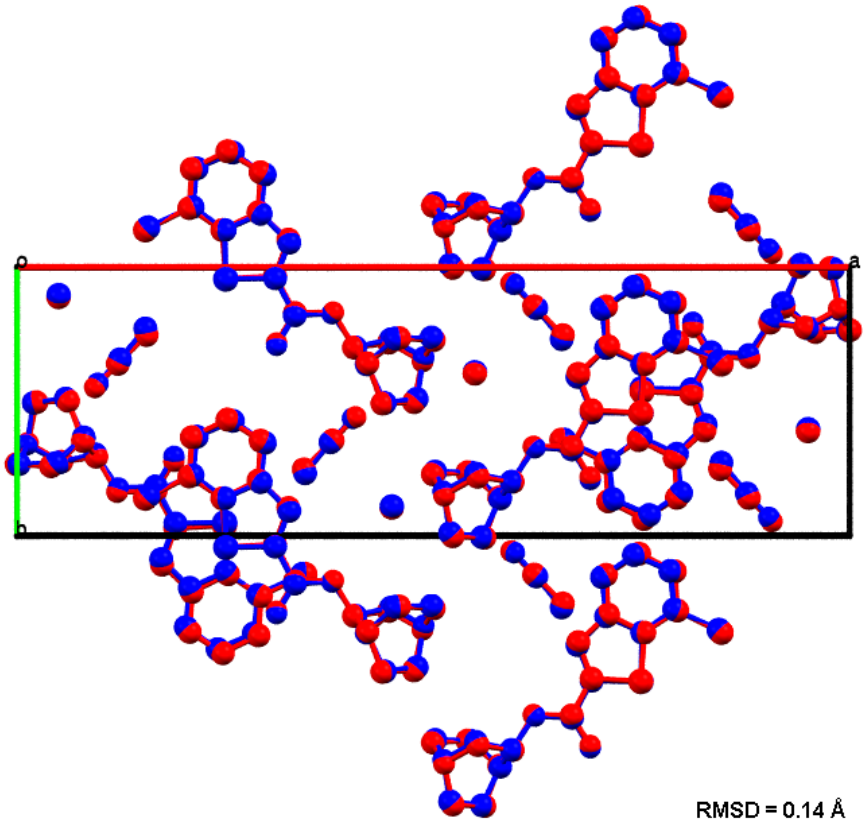


**Figure S27.** Overlay of form $S_{ACN\text{-}II}$ crystal structure calculated from PXRD data (blue) and crystal structure after DFT optimisation (red) with given $RMSD_{15}$ value for non-hydrogen atoms.

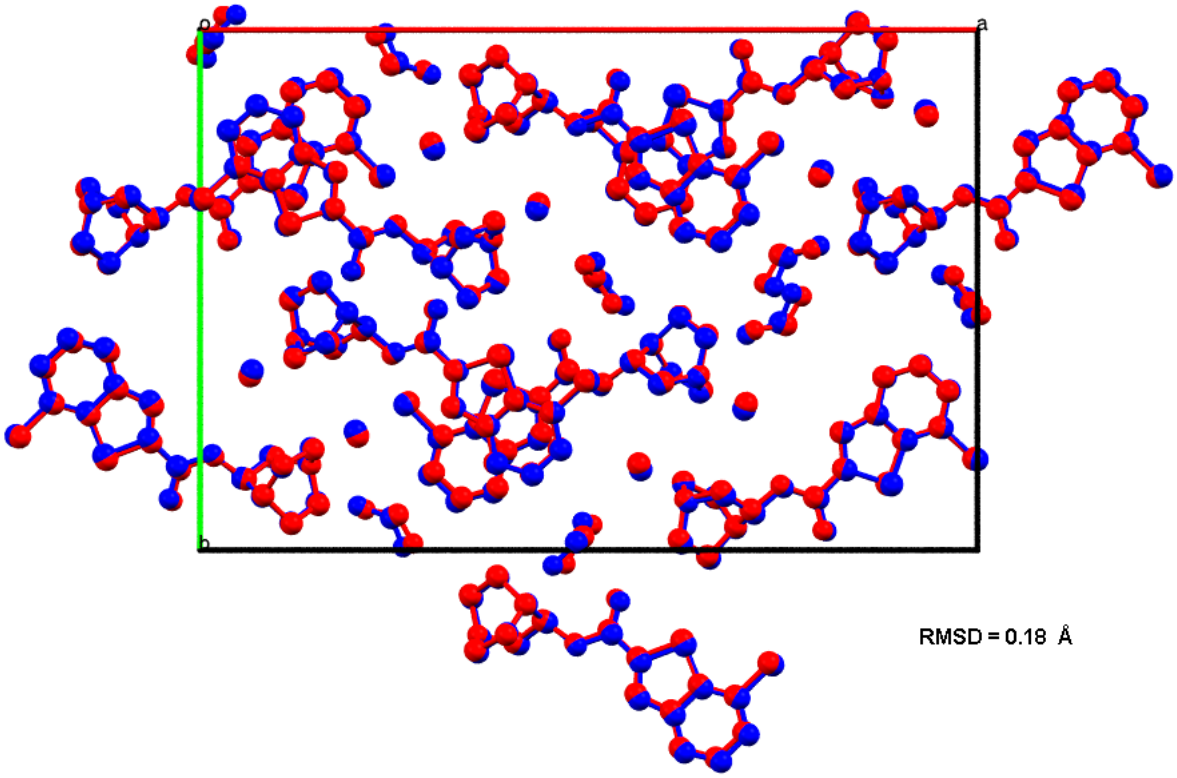


**Figure S28.** Overlay of form $S_{FA}$ crystal structure calculated from PXRD data (blue) and crystal structure after DFT optimisation (red) with given $RMSD_{15}$ value for non-hydrogen atoms.

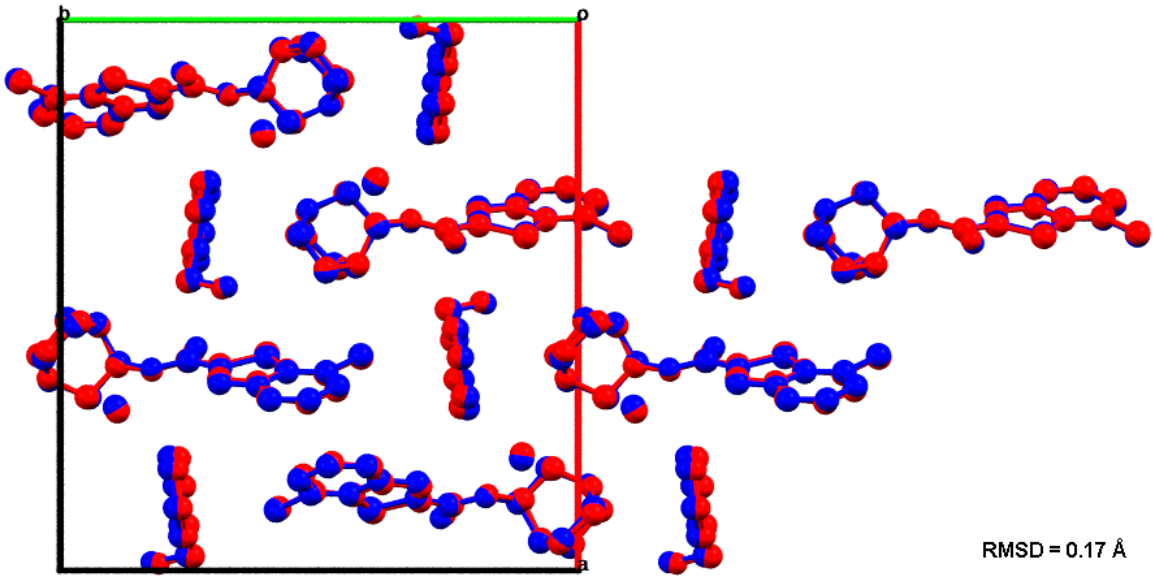


**Figure S29.** Overlay of form $S_{BnOH}$ crystal structure calculated from PXRD data (blue) and crystal structure after DFT optimisation (red) with given $RMSD_{15}$ value for non-hydrogen atoms.

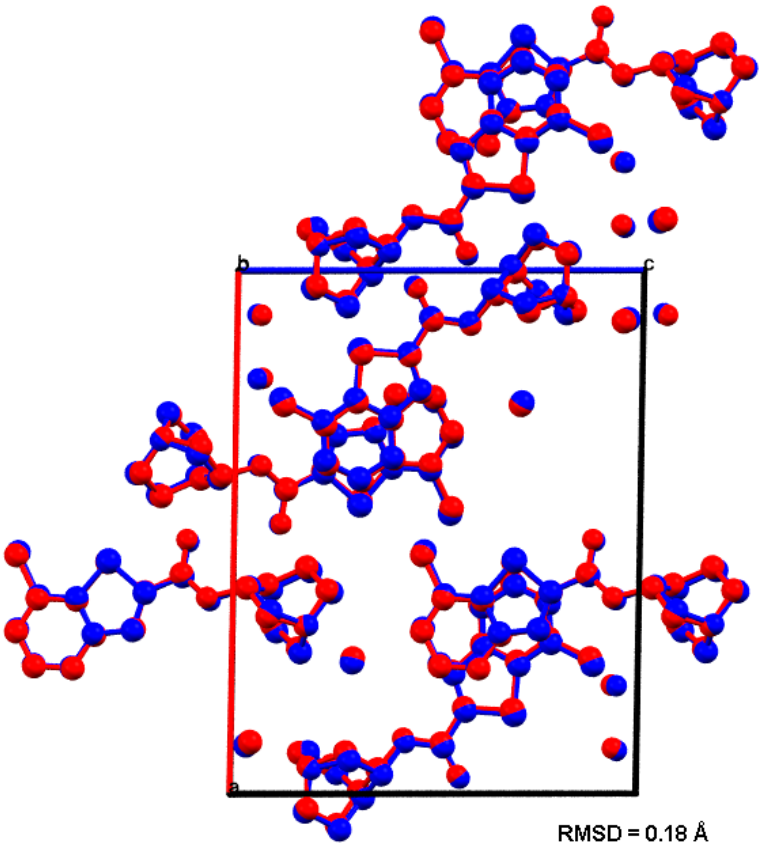


**Figure S30.** Overlay of form MH-V crystal structure calculated from PXRD data (blue) and crystal structure after DFT optimisation (red) with given $RMSD_{15}$ value for non-hydrogen atoms.

## SI 5. Conformation analysis

**Table S4.** Enc-HCl cation conformation data.

| Phase/ Conformer | τ1 (C2-C1-C10-O11)/ ° | τ2 (C1-C10-N12-C16)/ ° | τ3 (C10-N12-C16-C15)/ ° |
|---|---|---|---|
| **$IV_D$** | -160.4 | 178.7 | 153.5 |
| **$V_D$** | -161.3 | 173.7 | 145.3 |
| **$VI_D$** | -176.3 | 179.4 | 159.9 |
| **$VII_DA$** | -173.1 | 169.3 | 157.2 |
| **$VII_DB$** | -178.6 | 176.6 | 164.7 |
| **$VIII_D$** | -171.1 | 167.6 | 148.2 |
| **$IX_DA$** | -178.9 | 170.7 | 159.8 |
| **$IX_DB$** | -175.7 | 172.9 | 148.8 |
| **$XII_D$** | -169.1 | 179.1 | 166.8 |
| **$DS_{AA}$** | -179.2 | 175.6 | 143.0 |
| **$S_{FA}A$** | -166.9 | 176.8 | 142.1 |
| **$S_{FA}B$** | -173.1 | 175.2 | 155.4 |
| **$DS_{ACN}$** | -178.0 | 175.7 | 141.8 |
| **$S_{ACN-I}$** | -150.8 | 170.8 | 144.3 |
| **$S_{ACN-II}$** | -178.6 | 179.2 | 155.1 |
| **$S_{IBA}$** | -177.8 | 177.4 | 153.8 |
| **$S_{EtOH}$** | -178.0 | 176.5 | 141.7 |
| **$S_{BnOH}$** | -173.1 | 176.8 | 148.4 |
| **Gas phase opt.** | -164.9 | 176.8 | 160.0 |

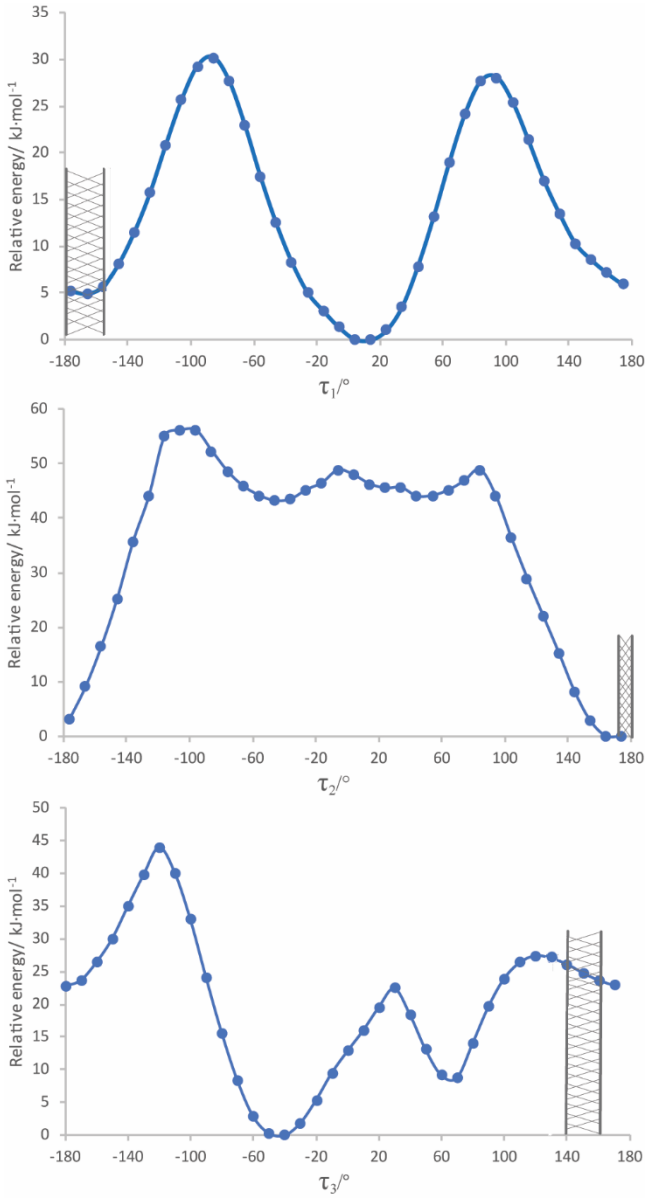


**Figure S31.** PES scans with respect to torsion angles $\tau_1$ – $\tau_3$ with marked interval of values observed in the experimental crystal structures.

**SI 6. Packing analysis**

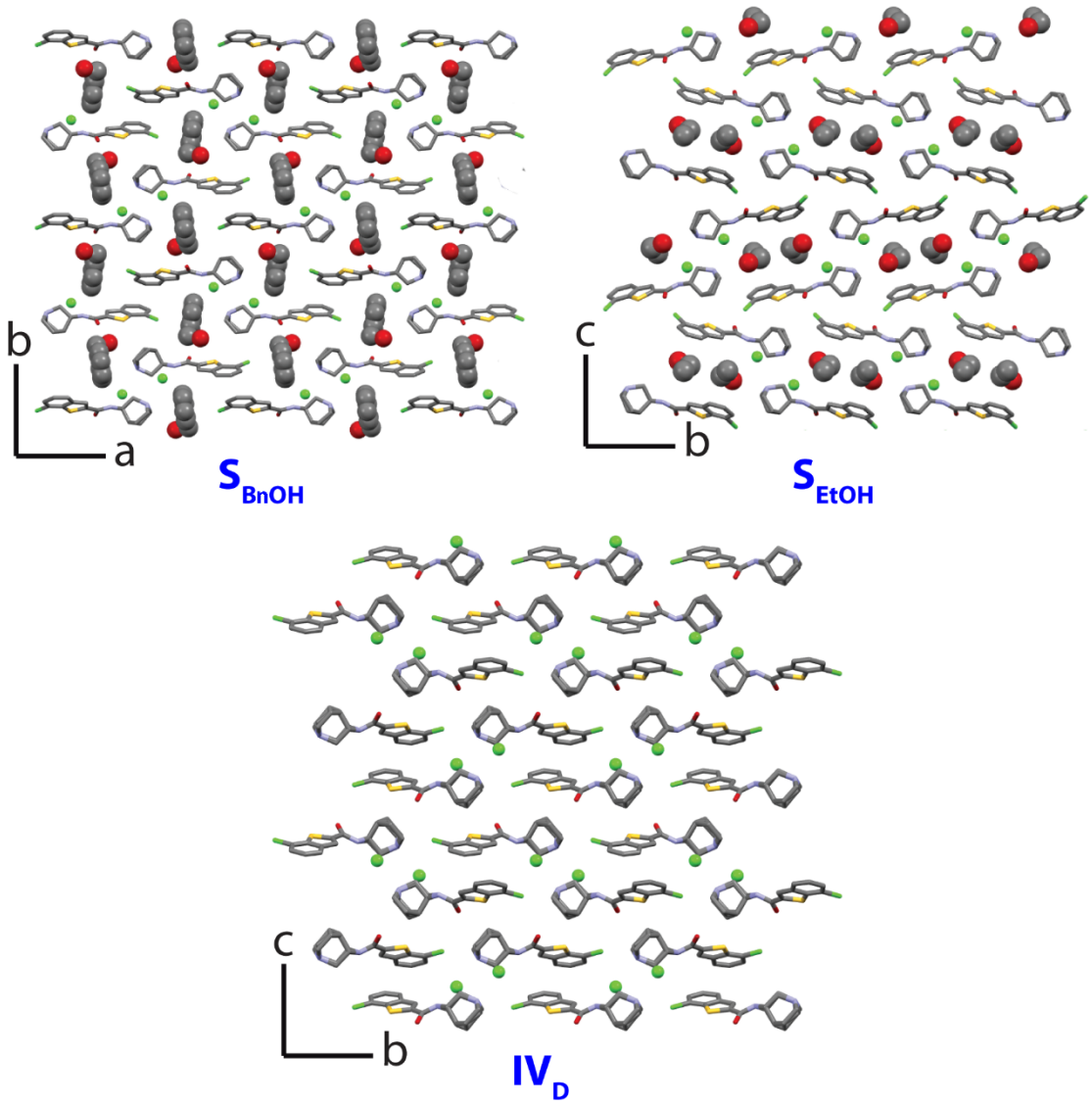


**S32.** Packing similarity between of Enc-HCl ethanol ($S_{EtOH}$), benzyl alcohol ($S_{BnOH}$) monosolvates and polymorph $IV_D$ with omitted hydrogens.

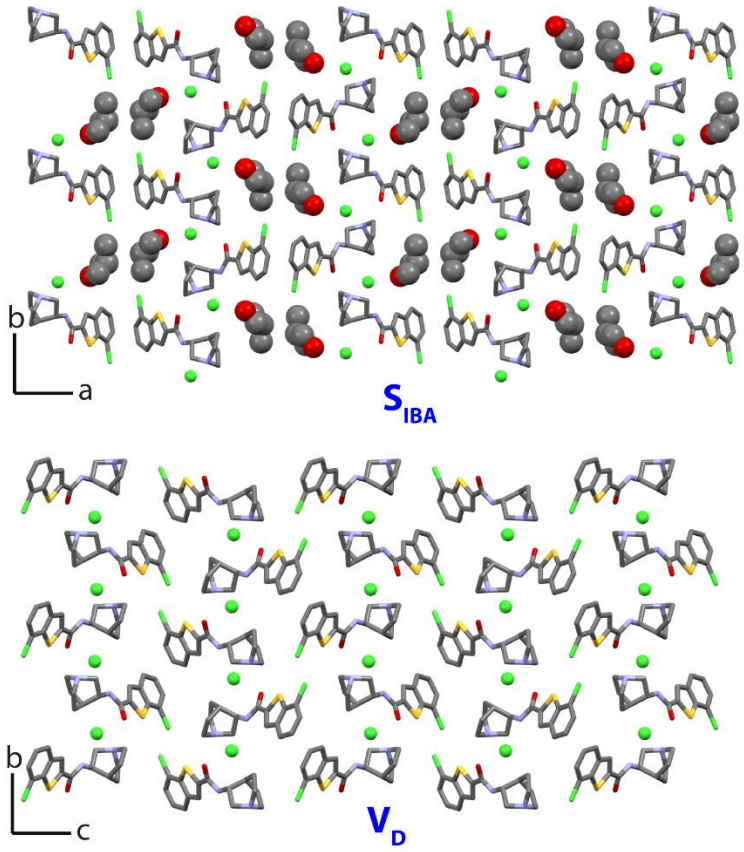


**S33.** Packing similarity between of Enc-HCl isobutanol monosolvate ($S_{IBA}$) and polymorph $V_D$ with omitted hydrogens.

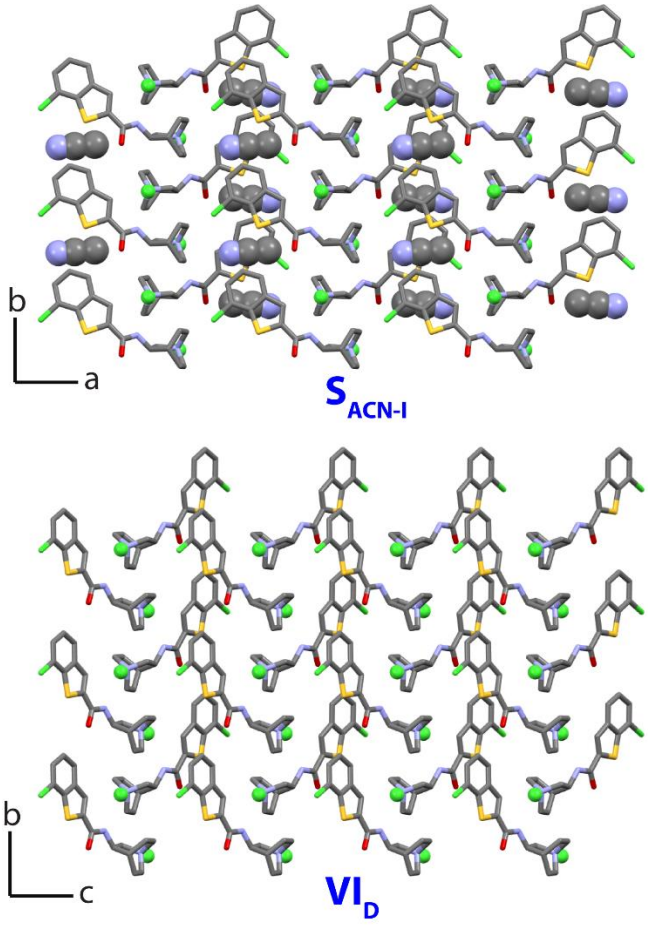


**S34.** Packing similarity between of Enc-HCl acetonitrile monosolvate 1 ($S_{ACN-I}$) and polymorph $VI_D$ with omitted hydrogens.

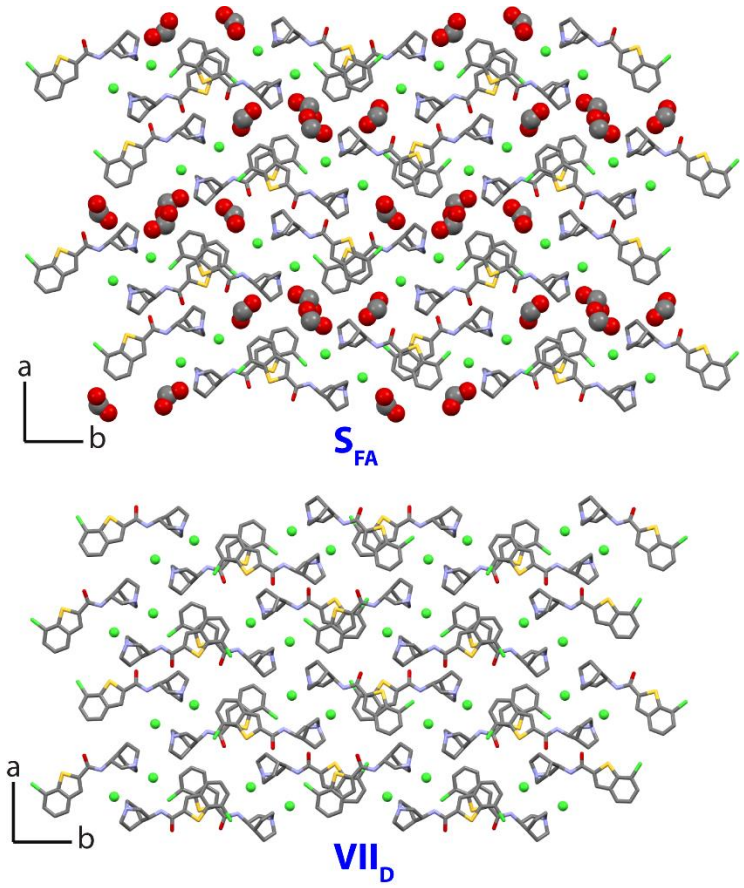


**S35.** Packing similarity between of Enc-HCl formic acid monosolvate ($S_{FA}$) and polymorph $VII_D$ with omitted hydrogens.

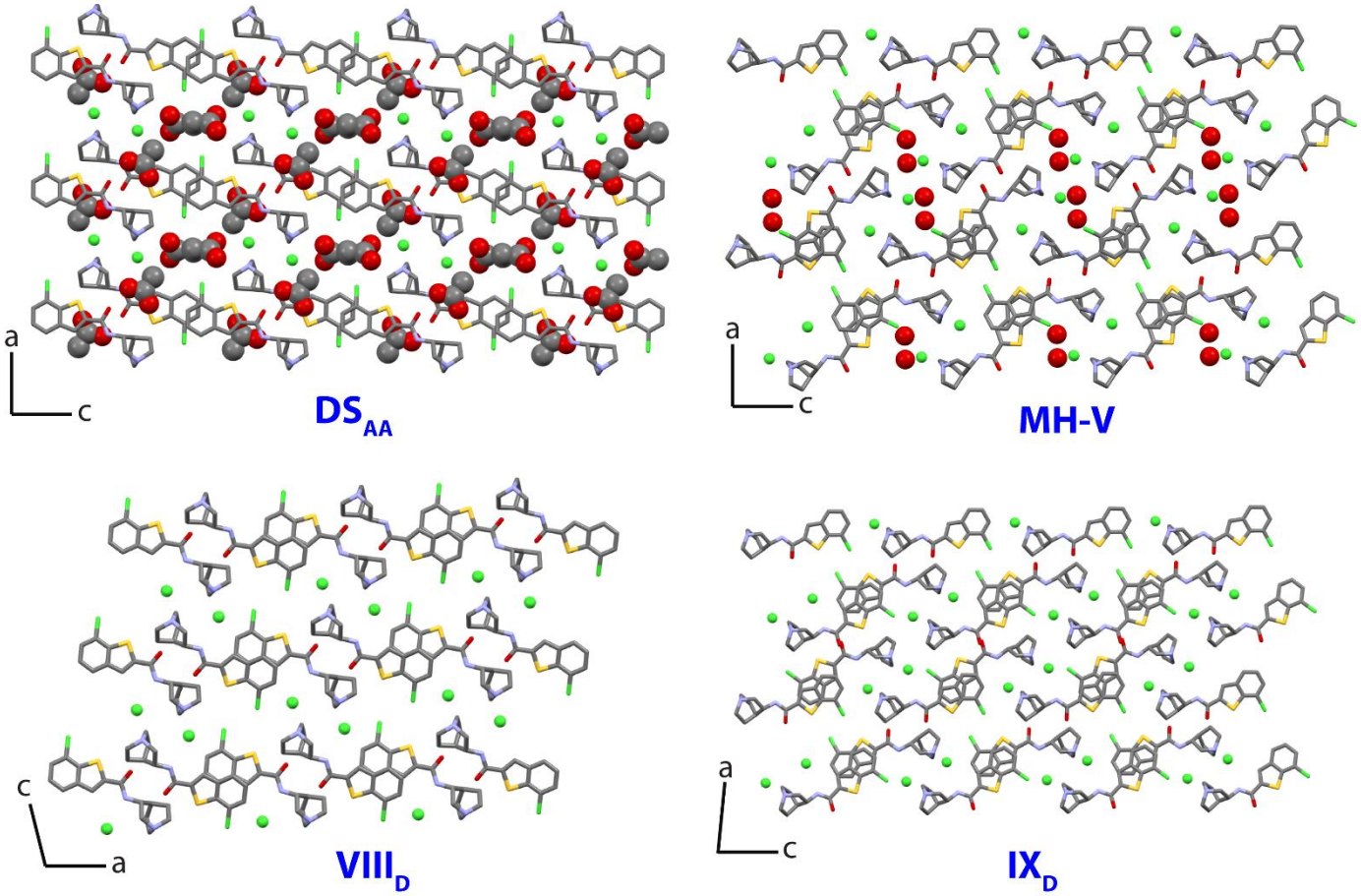


**S36.** Packing similarity between of Enc-HCl acetic acid disolvate ($DS_{AA}$), monohydrate (MH-V), polymorphs $VIII_D$ and $IX_D$ with omitted hydrogens.

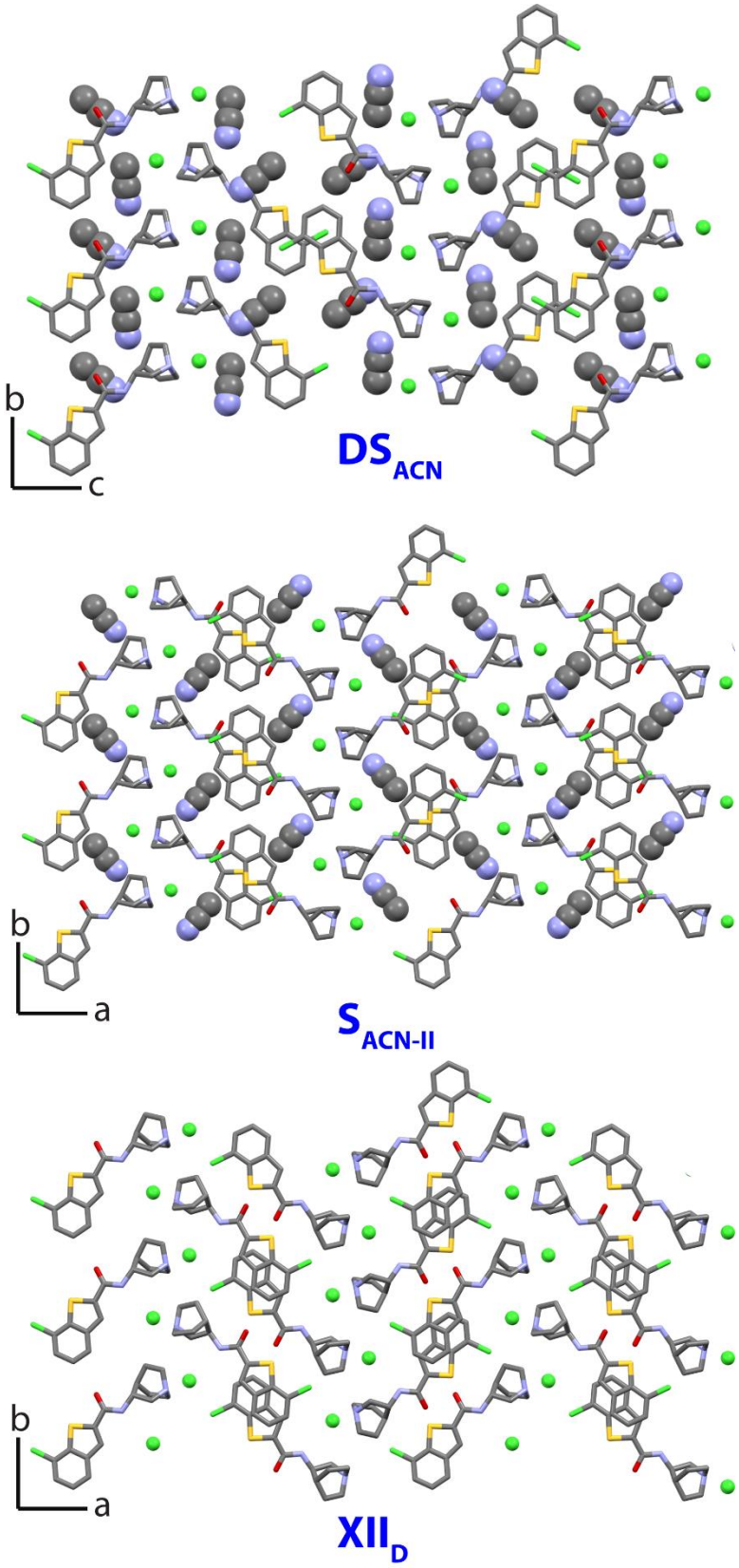


**S37.** Packing similarity between of Enc-HCl acetonitrile disolvate ($DS_{ACN}$), acetonitrile monosolvate 2 ($S_{ACN-II}$) and polymorph $XII_D$ with omitted hydrogens.

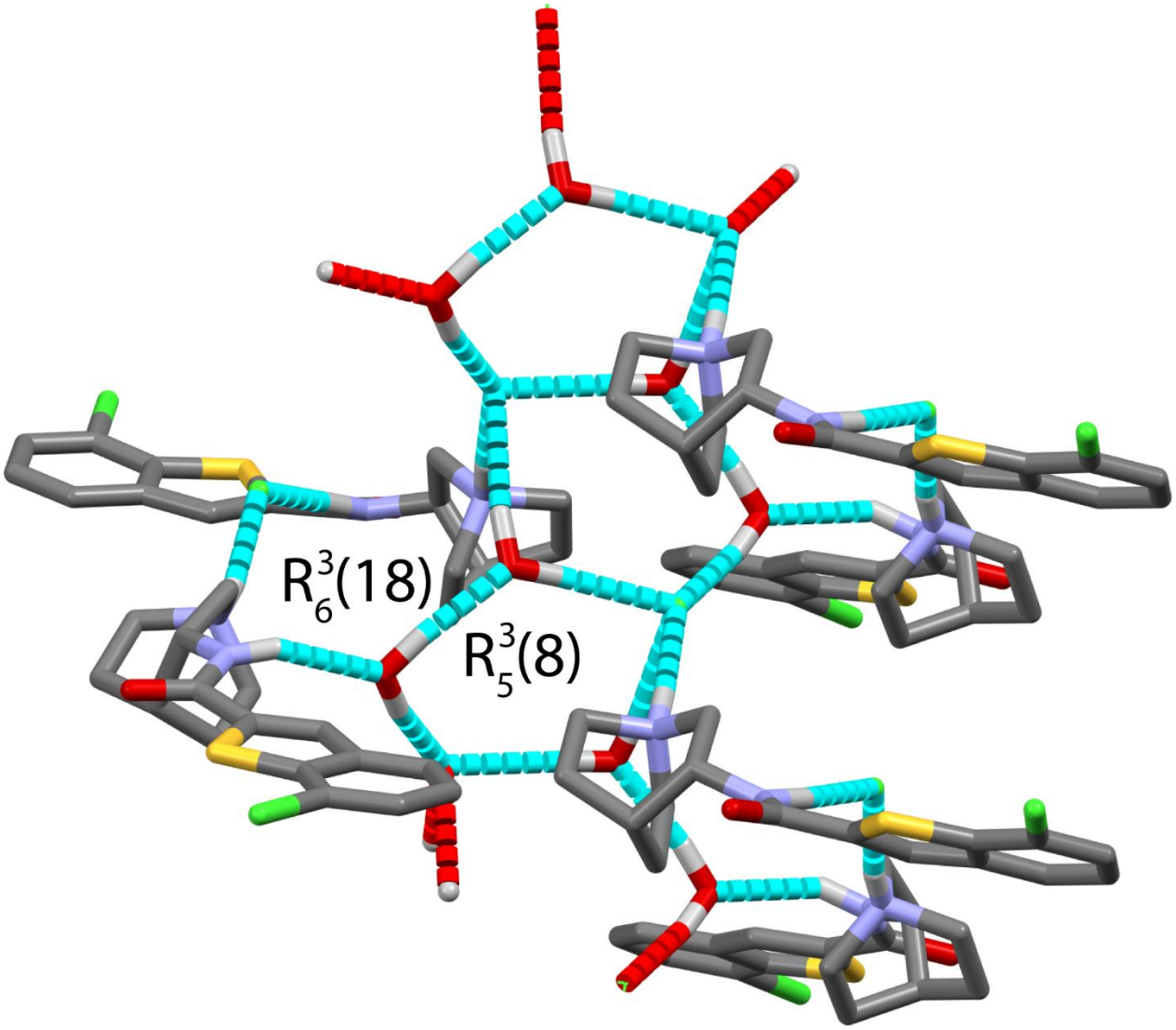


**S38.** Hydrogen bond network in Enc-HCl MH-V structure.